Chapter 4
The Seismic Structure of Island Arc Crust

A.J. Calvert

4.1 Introduction

Intraoceanic island arcs are considered to have been important building blocks in the formation of Earth's continental crust, with some of the oldest preserved crust created through amalgamation of island arcs and oceanic plateaux in the Middle to Late Archean, for example the Archean Superior Province of Canada (Hoffman 1989; Card 1990). Since the collision of island arcs with continental crust is presently occurring in locations such as Timor, Taiwan and northeastern South America, the addition of island arcs to existing continents is likely to have been a major contributor to continental growth throughout much of Earth's history. Studies of inferred arc terranes within continental regions can reveal much about the tectonic processes that incorporated arc crust into the continents, as well as some aspects of the original island arc crust, such as its age of formation; however, the lack of preservation of ancient, pre-collisional island arcs implies that we must look to modern islands arcs to understand many fundamental aspects of the island arc crust that became involved in past arc–continent collisions.

Modern ocean island arcs (Leat and Larter 2003) (Fig. 4.1 in Chap. 2) occur where one oceanic plate subducts beneath another whose stress state ranges from clearly extensional, such as the Tonga arc where back-arc spreading occurs, to neutral or mildly compressional such as the Aleutian arc (Jarrard 1986). Upper plates that are subject to a higher degree of compression are predominantly continental, though the Solomon arc, which is in collision with the Ontong Java plateau is an exception to this rule (Miura et al. 2004). In addition, some island arcs such as Japan have been built on, or contain some component of, remnant continental crust, and as such they cannot be considered pure island arc systems. In this paper, I will contrast the crustal structure of non-extended and extended island arc systems, including in the latter the inactive remnant arcs that are generated by arc rifting and separated from the active arc by back-arc spreading. Given the same magmatic input, an arc that is subject to one or more episodes of back-arc rifting will contain thinner crust than an arc that has not been so affected. This variation in the thickness of present-day island arc crust is one observation that will be emphasised due to its influence on the process of arc–continent collision and the resultant preservation of arc crust.

4.2 Island Arc Regimes

Metamorphic dehydration reactions within the subducted oceanic lithosphere release water into the overlying mantle wedge, generating melts that rise to form arc volcanoes, which define the location of the magmatic axis of the active arc (Stern 2002). The magmatic arc massif, whose abrupt seaward limit defines the magmatic front, averages approximately 100 km in width over all subduction zones (d'Ars et al. 1995), and is largely below sea-level in island arc settings. Volcanism can extend into the back-arc region, resulting in a less well-defined transition from arc to back-arc. The forearc lies between the magmatic front and the trench, and in the case of accretionary convergent margins will grow through

A.J. Calvert
Department of Earth Sciences, Simon Fraser University, 8888 University Drive, Burnaby, BC V5A 1S6, Canada
e-mail: acalvert@sfu.ca

D. Brown and P.D. Ryan (eds.), *Arc-Continent Collision*, Frontiers in Earth Sciences,
DOI 10.1007/978-3-540-88558-0_4,

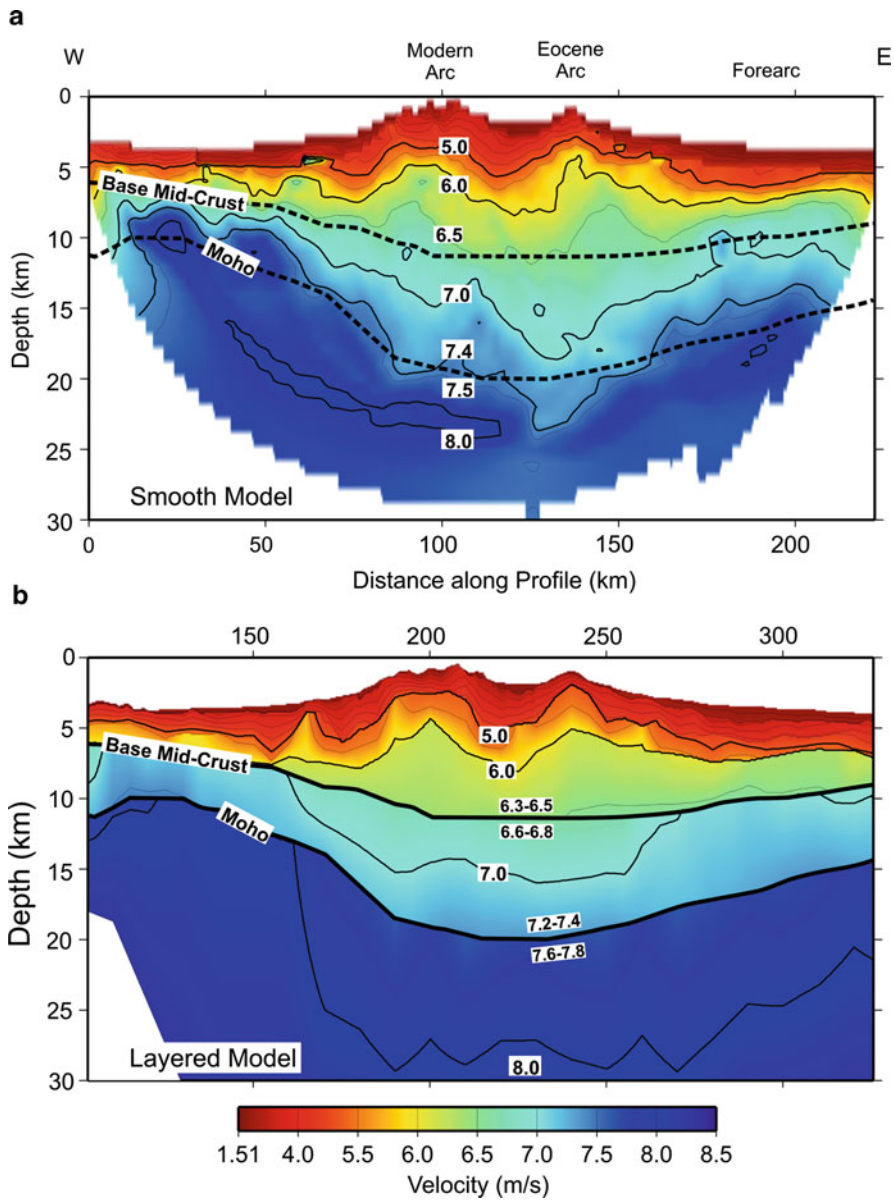

Fig. 4.1 Comparison of velocity models across the Mariana island arc. (**a**) Vertical section extracted from a 3D model derived using first arrival tomography. The 3D velocity model indicates that crustal velocities extend to greater depth beneath the frontal arc than the modern arc. (**b**) 2D velocity model obtained using first arrivals and wide-angle reflections from laterally continuous interfaces. The Moho and the base of the middle crust identified using wide-angle reflections (Takahashi et al. 2007) are shown by the *continuous heavy black lines*, and also indicated in (**a**) by *dashed lines*; the velocity contrasts across these interfaces are also shown. Vertical exaggeration is 4:1.

the addition of sediment, and perhaps igneous crust, scraped from the subducting plate to form an accretionary prism. In non-accretionary, and perhaps even accretionary settings, subduction erosion may remove material from the seaward edge of the forearc by slumping into the trench or from the base of the forearc crust (Von Huene and Scholl 1991). The width of the forearc averages 160 km (Gill 1981).

When the upper plate of an island arc system is under tension, back-arc basins form through the rifting

of the arc massif (Karig 1970), with the initial rift usually occurring within 50 km of the volcanic arc (Taylor and Karner 1983), which weakens the lithosphere due to its high heat flow and the presence of melt in a locally thickened crustal section (Molnar and Atwater 1978; Kuzsnir and Park 1987). Although arc rifting primarily occurs on the back-arc side of the arc, it can also be centered on the arc, or even in the forearc, resulting in the latter case in the two magma sources, associated with subducting slab and upwelling asthenosphere, migrating past one another as back-arc spreading develops (Martinez and Taylor 2006). When rifting occurs on the back-arc side of the arc massif, the remnant arc separates from the still unified magmatic arc and forearc through back-arc spreading. In this situation, the remnant arc will be quite narrow, and may not include any of the original volcanic edifices, e.g. the Kyushu-Palau Ridge (Kobayashi et al. 1995; Nishizawa et al. 2007). When rifting is centered on the arc volcanoes, as occurred in the Mariana arc, arc volcanism is greatly attenuated by the interaction between the different magmatic sources, but the arc will reestablish itself at the appropriate location above the slab as the back-arc spreading centres migrate away (Hussong and Uyeda 1981). If rifting occurs in the forearc, then the remnant arc will be uncommonly wide as seems to be the case with the Lau Ridge west of the Tonga-Kermadec subduction zone, and the active magmatic arc must shut down and reestablish itself closer to the trench as the back-arc basin opens (Martinez and Taylor 2006). Thus remnant arcs, which are typically identified by their associated seafloor ridges, can vary significantly in width and crustal thickness depending on the rifting process that created them.

Over the last 50 years, island arcs have been subject to a broad range of geoscientific studies, with recent emphasis on geochemical cycling through the subduction system and the magmatic evolution of the arc. One specific focus of interest has been the estimation of the volume of andesitic crust within the arc, because such crust has a similar composition to continental crust, and the widespread existence of such crust within island arcs would imply that arcs can indeed be the building blocks of continental crust. Although tonalitic rocks have been exhumed, for example, in the Tanzawa collision zone in Japan (Nitsuma 1989; Kawate and Arima 1998), seismic refraction surveys are required to constrain the subsurface distribution of such rocks in modern arcs from the inferred seismic velocities. In addition, seismic surveys can constrain the thickness of arc crust, and the vertical extent of the crust–mantle transition. In terms of arc–continent collision, crustal thickness and composition, which is closely related to density, are two key characteristics of arc crust that help determine the evolution of the process.

4.3 Seismic Studies of Arc Crust

Seismic refraction surveys of island arcs date back at least 40 years, and the early results, which include the Aleutian (Grow 1973), Kurile (Gorshkov 1970), Izu-Bonin-Mariana (Murauchi et al. 1968), New Britain (Wiebenga 1973) and Tonga-Kermadec (Shor et al. 1971) arcs are summarized by Gill (1981). These surveys indicated a 6–9 km thick upper crustal layer with P wave velocities of 5.0–5.7 km s^{-1} overlying a 10–15 km thick lower crust with velocities of 6.5–7.0 km s^{-1}. The P wave velocities of the deepest, underlying layer varied from 7.5–8.2 km s^{-1}, raising some uncertainty about whether values less than 7.8 km s^{-1} in fact represented lowermost arc crust or uppermost mantle. As an alternative to a sharp crust–-mantle transition, Jacob and Hamada (1972) used surface wave data from earthquakes to postulate the existence of a crust–mantle transition zone between 20 and 40 km depth beneath the Aleutian arc, and this issue remains relevant today. These early seismic refraction results demonstrated the first order characteristics of much arc crust, namely a 15–25 km thick crust and the absence of a thick, laterally continuous layer with velocities of approximately 6.1 km s^{-1}, as commonly found in continental interiors (Christensen and Mooney 1995).

Seismic surveying and data analysis techniques have evolved significantly over the last two decades, and densely sampled 2D profiles and 3D areal surveys can now constrain well 20 km wide lateral velocity variations in middle and lower arc crust, e.g. Takahashi et al. (2007) and Calvert et al. (2008). With this degree of resolution, modern seismic surveys have reached the point where lateral velocity variation (a proxy for compositional variation) in the middle crust can be correlated with geochemical variations in surface volcanoes (Kodaira et al. 2007a). This paper reviews the seismic structure of two island arcs that represent end members of the present-day spectrum of island arc

systems, because they have been recently studied using modern seismic techniques:

1. Aleutian arc: initiated in the Eocene and not significantly affected by extension and arc rifting
2. Izu-Bonin-Mariana arc-back-arc system: initiated in the Eocene and variably affected by localised extension plus two episodes of arc rifting and back-arc spreading, which have produced two remnant arcs now separated from the modern magmatic arc

These seismic surveys reveal the degree of along-strike variability of both active and remnant arcs, both of which can eventually become involved in arc–continent collision. The seismic structure of the southern part of the Lesser Antilles arc is also presented to demonstrate the effect of late sedimentary input as an arc approaches and collides with a continent.

In addition, the average variation of seismic P wave velocity with depth is derived for several recently surveyed island arcs. These individual velocity functions and a global average for all island arcs are contrasted with the average velocity variation of continental crust.

4.3.1 Seismic Methodologies and Model Comparisons

The seismic velocity models included in this paper come from different seismic refraction surveys, and more importantly, have been analysed using different techniques. Therefore, a general understanding of these methods will help to explain the different characteristics of the velocity models presented, and facilitate comparisons between them. Seismic surveys of island arcs are predominantly marine with land recording on the islands. Recent field surveys have comprised closely spaced (50–250 m) airgun shots recorded by sparsely distributed receivers usually spaced at larger intervals of 5–30 km along an approximately linear profile. All velocity models shown here have essentially been derived from the arrival times of two types of seismic wave: diving (refracted) arrivals that turn in the subsurface as they propagate directly from source to receiver and arrivals reflected upward at wide-angle from relatively sharp, flat to shallowly dipping boundaries in the crust.

Diving waves are relatively easy to identify in field data, at least at shorter source–receiver offsets (<50–100 km), because they are mostly first arrivals. P wave velocity models can be derived by tomographic inversion of first arrival travel times alone, and although there are a variety of approaches, those methods frequently used in crustal seismology produce velocity models that vary smoothly both in depth and laterally; the sharp changes in velocity that occur at the top of the igneous crust or at the Moho tend to be smoothed out.

The additional inclusion of wide-angle reflections can improve the resolution of velocity models, because the existence of a reflection requires a relatively sharp change in seismic velocity. This information can be incorporated into the velocity model by including laterally continuous interfaces across which the seismic properties suddenly change. In many crustal velocity models, these interfaces are continuous for 100 km or more, producing characteristically layered models. Figure 4.1 contrasts the greater lateral variability of a velocity model derived by first arrival tomography (Zelt and Barton 1998) with a layered model, in which wide-angle reflections have been included (Zelt and Smith 1992). Since wide-angle reflections are secondary arrivals, their identification can be influenced by various types of noise and the sparse distribution of the recording instruments. Thus the reflection points of the identified wide-angle reflections do not usually extend over the full length of the interfaces included in most velocity models. Essentially, improved vertical resolution in the model is obtained at the cost of including parts of an interface from which no reflections have been identified, raising the possibility that this section of the interface may not exist; the constraint of an interface can, however, be assessed from the distribution of reflecting points along the boundary. An alternate approach to determining where interfaces should be introduced into the velocity model is to locate, or "migrate", reflection arrival time picks in the distance-depth domain of the model using velocities derived only from a tomographic inversion of first arrivals (Ito et al. 2005; Fujie et al. 2006). The envelope of these migrated picks indicates the position and degree of lateral continuity of subsurface reflectors.

In the following examples of seismic velocity models, only the first order characteristics of the models that would likely be well-constrained by any travel

time inversion approach are discussed. A general description of the constraint of the velocity models is presented, but the reader is referred to the original publications for full details of ray coverage, model assessment procedures and checkerboard tests.

4.4 Aleutian Arc

4.4.1 Tectonic History

The present-day Aleutian arc, which developed in the Eocene, extends 3,000 km from the Kamchatka peninsula in the west to the Gulf of Alaska in the east (Fig. 4.2). Unimak Pass at the southwestern end of the Alaska Peninsula marks the eastward transition from subduction of the Pacific Plate beneath oceanic lithosphere attached to the North America plate to subduction beneath accreted terranes and continental crust. Along the oceanic part of the subduction zone, convergence varies from 6.3 cm yr^{-1} to the NNW in the east to 7.4 cm yr^{-1} towards the NW in the west (DeMets and Dixon 1999). Due to the arcuate geometry of the trench, the relative velocity vector changes from almost trench-normal in the Gulf of Alaska to almost trench-parallel in the west.

At approximately 60 Ma, the Kula plate was subducting beneath the Beringian and southwestern Alaskan margins, which both included the Peninsula and Chugach terranes, corresponding respectively to the arc and forearc of the accreted Jurassic Talkeetna arc complex (Plafker et al. 1994). Between 56 and 42 Ma, a series of southward and westward jumps in the location

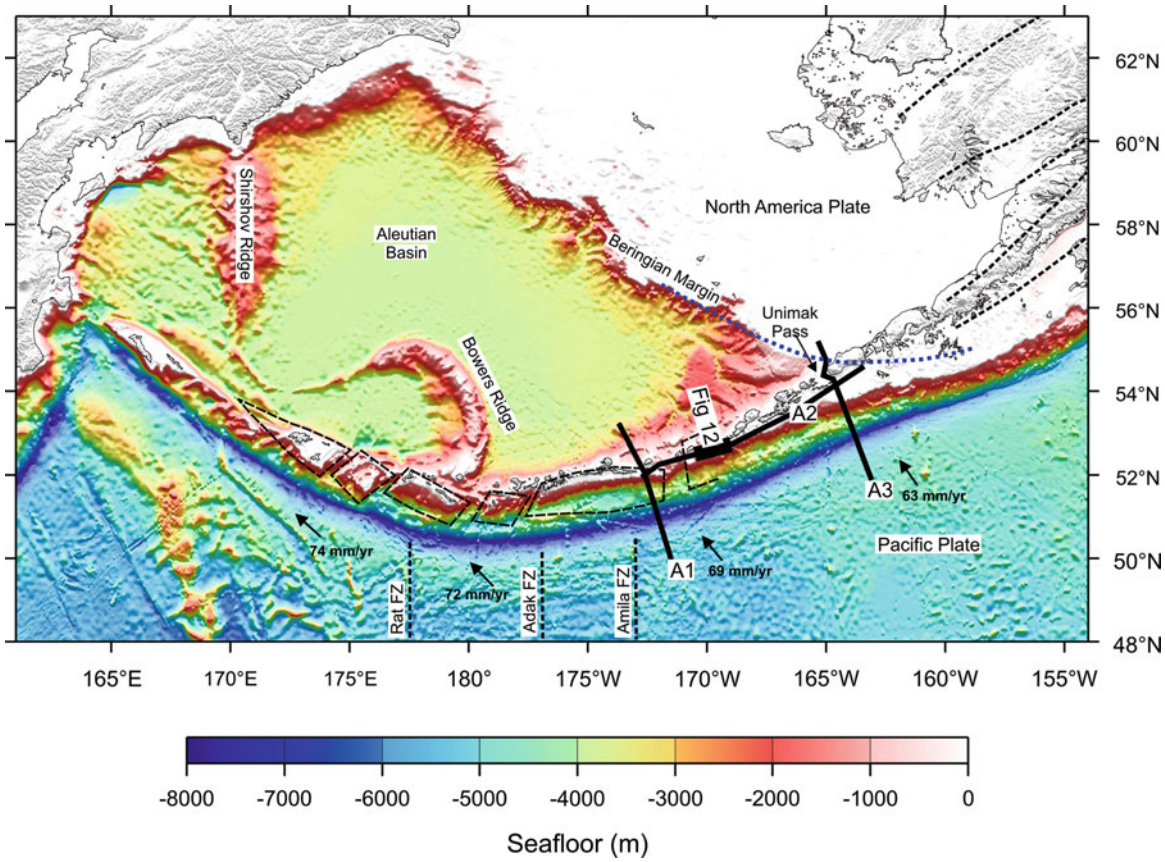

Fig. 4.2 Bathymetry of the Aleutian arc showing the location of the three lines acquired as part of the 1994 survey. *Long dashed black lines* indicate the segmentation and block rotation along the arc (Geist et al. 1988). The transition from an oceanic to a continental style of subduction occurs near Unimak Pass, and the *blue dashed line* shows the inferred location of the Beringian margin (Lizarralde et al. 2002). *Short black dashed lines* on the Pacific plate show the location of fracture zones. The convergence rate and direction at the trench is indicated by the *arrows*. Seafloor depth scale is the same as in Fig. 4.1 of Gerya in Chap. 2.

of subduction trapped a large remnant of the Kula plate against the North American plate, transforming the Beringian margin into a passive margin, and creating to the south an intraoceanic subduction zone where the Pacific plate now subducts beneath oceanic lithosphere of the former Kula plate (Scholl et al. 1992; Plafker and Berg 1994). Lizarralde et al. (2002) used seismic and potential field data to infer that the southward limit of the former Beringian margin lies just north of the Alaskan peninsula near Unimak Pass (blue dashed line in Fig. 4.2). In the oceanic section of the subduction zone, the full width of the arc massif is segmented along strike into blocks that have been subject to clockwise rotation (Geist et al. 1988).

4.4.2 Seismic Survey

Three wide-angle seismic profiles were shot over the Aleutian island arc (Fig. 4.2) by the *R/V Ewing* in 1994 using an airgun array with a total volume of 8,400 in^3:

- Line A1 was located across the oceanic part of the arc and employed 14 ocean-bottom seismometers (OBS) spaced every 20 km over the arc massif (Holbrook et al. 1999)
- Line A2 was more sparsely recorded along the inner forearc by effectively ten land stations and two OBS that were spaced 20–120 km apart and offset 20–60 km from the airgun line (Fliedner and Klemperer 1999)
- Line A3 was acquired across the arc at Unimak Pass using 16 OBS spaced 15–30 km apart (Lizarralde et al. 2002)

Although line A3 is approximately located at the along-strike transition from the oceanic to the continental arc, the interpretation of the former Beringian margin close to the northern end of this line implies that most of line A3 is located over arc crust with an oceanic affinity (Lizarralde et al. 2002).

4.4.3 Seismic Velocity Models

4.4.3.1 Cross-Arc Lines

On lines A1 and A3, diving rays, intracrustal reflections, and PmP reflections from the arc Moho plus a few reflections from the top and occasionally bottom of the subducting oceanic crust were identified in the wide-angle seismic data. P wave velocity models for lines A1 (Holbrook et al. 1999) and A3 (Lizarralde et al. 2002) were both derived by 2D travel time inversion of the wide-angle data with some additional travel times from normal incidence data using the methodology of Zelt and Smith (1992). In both models, the arc crust is divided into five layers, with three layers corresponding to the upper crust, separated by laterally continuous interfaces across which velocity discontinuities are present (Fig. 4.3). The crust is 25–32 km thick below the arc massif, but thins across the forearc to 12–15 km where the mantle wedge terminates towards the trench. On line A3, the upper and middle crust are generally well-constrained by both diving rays and wide-angle reflection raypaths. The arc Moho is located by PmP reflections under the arc massif, but the depth of the Moho is only inferred below the forearc. The position of the subducting oceanic crust is constrained by both normal incidence and wide-angle reflections south of the trench. Under the arc massif the subducting oceanic crust has been inserted into the model to be consistent with a small number of reflections and the Wadati-Benioff seismicity; below 20 km depth, the subducting crust is probably not well-located by the wide-angle survey alone.

The crustal architecture of the arc massif inferred for lines A1 and A3 is generally similar. Beneath a layer of volcaniclastic sediments of variable thickness, the upper igneous arc crust exhibits P wave velocities of 4.0–5.9 km s^{-1}, and the middle crustal layers have velocities of 6.5–6.9 km s^{-1}. The thickening of the mid-crustal layer on line A3 just seaward of the volcanic line may be linked to imbrication in the more complex tectonic environment at the tip of the Alaskan peninsula. The 12–20 km thick lower crust has velocities of 6.9–7.5 km s^{-1}; this lower layer thins under the forearc where it exhibits the highest velocities: 7.2 km s^{-1} on line A1 and 7.5 km s^{-1} on line A3. Neither line across the arc provides evidence for a significant volume of arc crust with velocities of 6.0–6.5 km s^{-1}.

4.4.3.2 Along-Strike Variation

Velocity models derived from seismic profiles acquired across an island arc may not always be representative of the arc along its full length due to the locations selected, and lines along the strike of the arc, such as

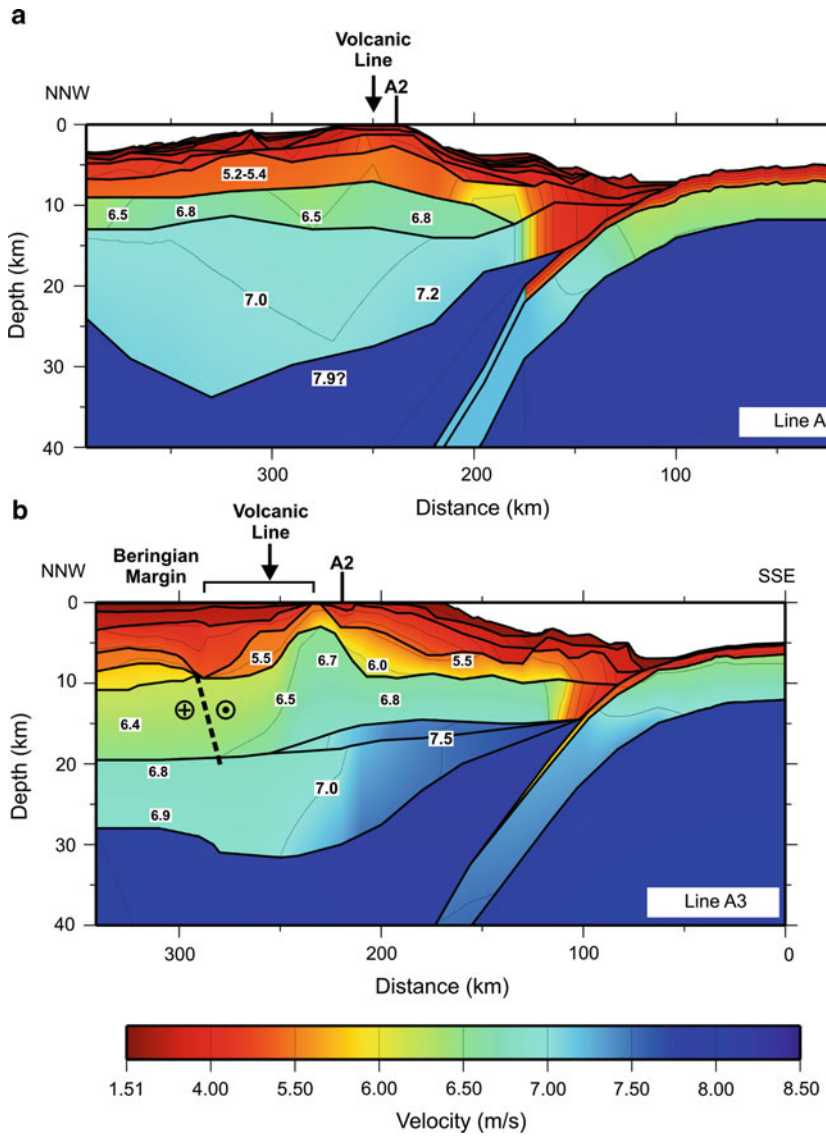

Fig. 4.3 Seismic velocity models across the Aleutian arc. (**a**) Western line A1 across the oceanic part of the arc (Holbrook et al. 1999); (**b**) Eastern line A3 in the region where the Aleutian arc changes from oceanic to continental (Lizarralde et al. 2002). The two velocity models are aligned at the location of the trench. The former Beringian margin, which may have been largely strike-slip late in its history, is shown by the *dashed black line* towards the NNW end of line A3. The upper plate crust to the south probably comprises relict Kula oceanic crust and overlying accretionary complex. The bar above line A3 marks the section of the line that was deviated around Unimak island. Vertical exaggeration is 4:1.

line A2, can identify anomalous regions that would not otherwise be detected. Due to the offset by 20–60 km of land receivers from the line of airgun shots, the travel times of diving rays and wide-angle reflections picked along line A2 were initially inverted by Fliedner and Klemperer (1999) using a 3D methodology (Hole 1992; Hole and Zelt 1995). However, the sparse distribution of the sources and receivers is more amenable to a 2.5-D inversion approach, in which ray-tracing is carried out in three dimensions, but the velocity structure is not allowed to vary perpendicular to the arc (van Avendonk et al. 2004). Using a tomographic velocity model from first arrivals recorded by a 4.2 km towed hydrophone streamer in the simultaneous normal incidence survey to fix the shallow structure, a velocity model was derived for 800 km

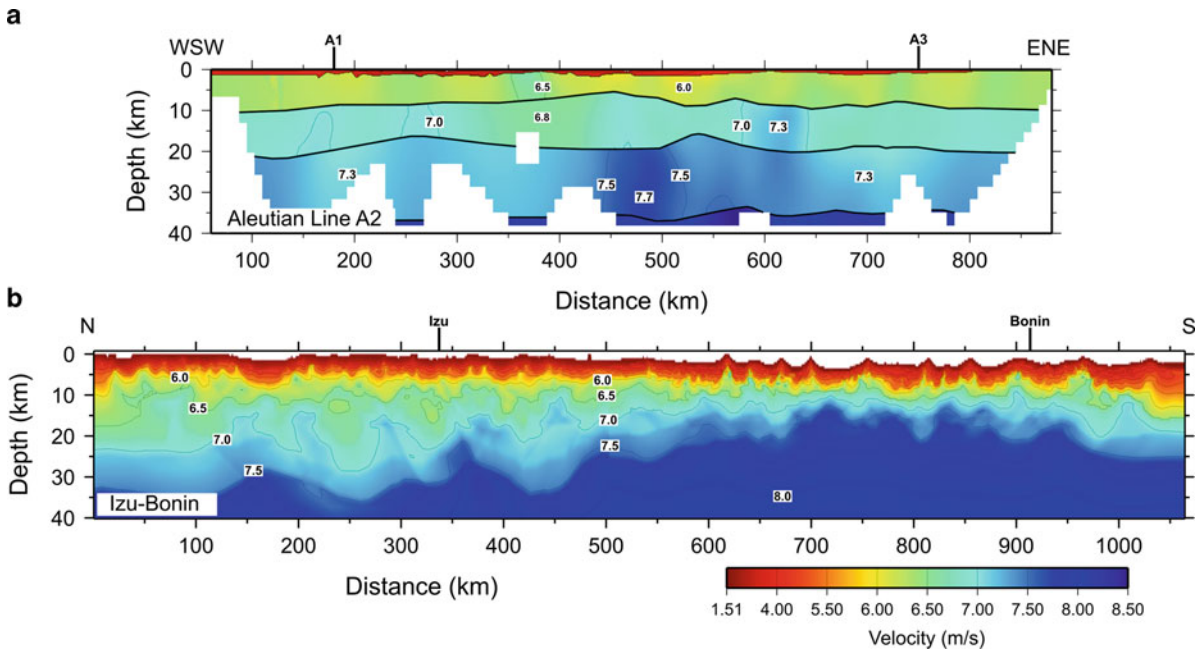

Fig. 4.4 Seismic velocity models along the Aleutian and Izu-Bonin arcs. (**a**) Line A2 is located over the inner forearc (Shillington et al. 2004); (**b**) Combined velocity models along the modern volcanic line of the Izu and Bonin arcs (Kodaira et al. 2007b). Velocities are displayed with the same scale as Fig. 4.3. Vertical exaggeration is 4:1.

along the strike of the arc (Fig. 4.4a) including the intersections with lines A1 and A3 (Shillington et al. 2004). In this model, the interfaces required to reproduce the arrival times of wide-angle reflections define three layers corresponding to the igneous arc crust, which is approximately 35 km thick. The upper crust is characterized by relatively high P wave velocities of 6.0–6.5 km s^{-1}; velocities are 6.5–7.3 km s^{-1} in the mid-crustal layer, and 7.3–7.7 km s^{-1} in the lower crustal layer.

Some differences in the crustal thickness and model velocities at the intersections of line A2 with the orthogonal profiles, A1 and A3, can be observed; for example, the crust is approximately 27 and 30 km thick on lines A1 and A3 respectively versus 35 km on the strike line A2 at the corresponding locations. Line A2 exhibits higher velocities throughout the crust than either line A1 or A3 at the same depth. This is most evident in the upper crust at a depth of ~5 km where there is a discrepancy of ~0.9 km s^{-1}, which diminishes to <0.2 km s^{-1} near the base of the crust. The discrepancy in the shallow velocities is attributable to the additional incorporation into line A2 of well-constrained velocities inferred from refractions recorded by the towed hydrophone streamer. Differences in deeper velocities may be attributable to an easier identification of wide-angle reflections on line A2 where the seafloor varies little; however, the sparse receiver distribution along line A2 introduces some uncertainty in the continuity of interfaces along strike. The intersections with lines A1 and A3 also occur near the ends of line A2 where only unreversed phases are present and the ray density is low (Shillington et al. 2004). In addition, the 3D structure of the arc, which cannot be resolved in this sparse survey, represents an additional source of uncertainty.

4.5 Izu-Bonin-Mariana Arc-Back-Arc System

4.5.1 Tectonic History

The Izu-Bonin(Ogasawara)-Mariana (IBM) subduction zone, along which Late Cretaceous to Early Jurassic ocean crust of the Pacific plate descends beneath the Philippine Sea plate, extends 2,800 km from Guam in the south to Japan in the north (Fig. 4.5), where the northern end of the volcanic arc is colliding with

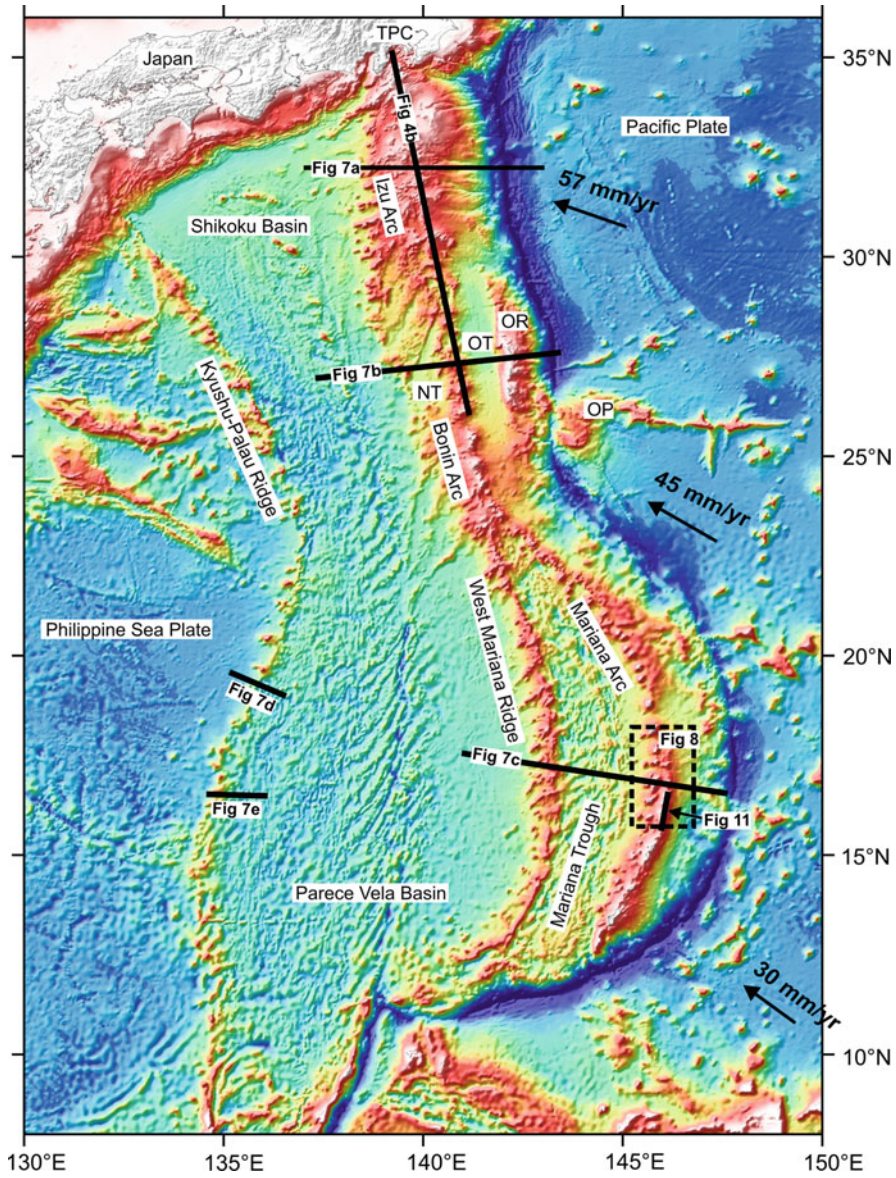

Fig. 4.5 Bathymetry of Izu-Bonin-Mariana arc-back-arc system with the location of seismic lines. The seismic lines are identified by their figure numbers within the chapter. The *dashed black rectangle* indicates the location of the 3D survey of Calvert et al. (2008). The convergence of the Pacific plate at the trench is indicated by the *arrows*. *OR* Ogasawara Ridge; *OT* Ogasawara Trough; *OP* Ogasawara Plateau; *NT* Nishinoshima Trough; *TPC* Tanzawa plutonic complex. Seafloor depth scale is the same as in Fig. 4.2.

the main Japanese island of Honshu (Stern et al. 2003). The convergence between these two plates varies between 2.4 cm yr^{-1} to the NW at 12°N to 6.1 cm yr^{-1} to the WNW at 34°N (Seno et al. 1993). A well-developed back-arc spreading centre exists west of the Mariana segment of the subduction zone, and estimates of the full spreading rate vary between 3.0 and 4.3 cm yr^{-1} (Bibee et al. 1980; Hussong and Uyeda 1981), implying that the convergence rate across the Mariana Trench is approximately 6–7 cm yr^{-1}. The strongly arcuate geometry of the Mariana segment of the subduction zone, which has arisen as a result of

back-arc spreading, implies oblique convergence along most of the trench with orthogonal convergence occurring only in the southern part of the Mariana arc system.

The IBM subduction zone was initiated in the Early Eocene (~50 Ma) (Fig. 4.6) (Taylor 1992; Stern and Bloomer 1992; Ishizuka et al. 2006), perhaps by the transformation to a trench of a fracture zone or weak line in the Pacific plate as a result of a change in the plate tectonic regime (Uyeda and Kanamori 1979). Early arc magmatism was characterized by boninitic magmas and very rapid crustal production rates until the modern-style island arc became established by the Late Eocene (~35 Ma) (Stern and Bloomer 1992). Early localised extension and partial rifting of the Bonin arc during the Eocene separated the Ogasawara ridge, which now forms part of the forearc (Ishizuka et al. 2006). In the Oligocene, rifting of the early arc began in the south at ~29 Ma and in north at ~25 Ma, and had developed along the entire IBM arc by 22 Ma (Taylor 1992, Kobayashi et al. 1995). Back-arc spreading along most of the IBM system up to 15 Ma created the Shikoku basin in the north and the Parece Vela basin in the south, which separated the remnant Kyushu-Palau ridge in the west from the still active IBM arc in the east (Hussong and Uyeda 1981; Kobayashi et al. 1995, Okino et al. 1999). The Mariana segment of the arc was subject to another rifting episode at ~8 Ma, with seafloor spreading commencing at 3–4 Ma (Bibee et al. 1980; Crawford et al. 1981). Back-arc spreading in the Mariana Trough continues, separating the West Mariana Ridge from the presently active Mariana arc that formed 3–4 Ma ago ~40 km west of the remnant Eocene arc (Fryer 1995; Stern et al. 2003). After 5 Ma, the rear side of the Izu-Bonin arc was also affected a by second episode of

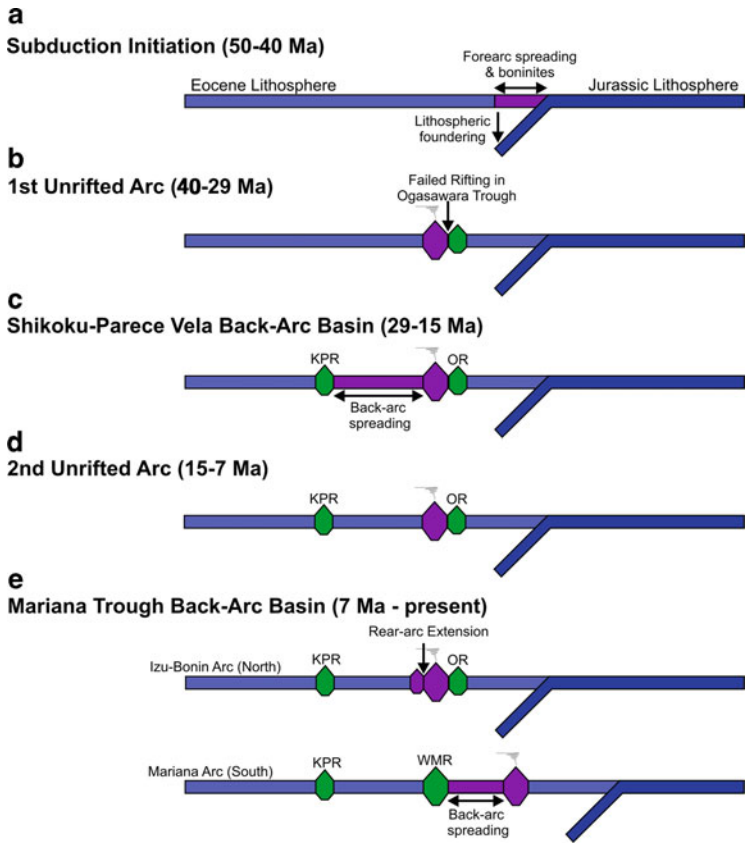

Fig. 4.6 Cartoon showing a simplified history of the Izu-Bonin-Mariana arc-back-arc system (after Stern et al. 2003). *Red* regions are currently or recently magmatically active; *green* areas represent inactive rifted arc crust. *OR* Ogasawara ridge, *KPR* Kyushu-Palau ride, *WMR* West Mariana ridge.

rifting, which created rift basins that have not yet developed into spreading centres (Taylor 1992).

The distance of the Mariana arc from continental areas has restricted the sedimentary input to the subduction zone to pelagic and volcaniclastic sediments. No significant accretionary wedge has developed because most of the incoming sediment is subducted and the forearc is also subject to erosion (Clift and Vannucchi 2004).

4.5.2 Seismic Surveys

More seismic surveys have been acquired over the IBM arc-back-arc system than any other island arc on Earth. Consequently it is possible to contrast seismic velocity models across the arc representing different evolutionary histories, and to constrain them with strike lines where available.

The Izu arc lies at the northern end of the IBM arc-back-arc system, and although affected by Oligocene arc rifting early in its history, the seafloor is shallower than 2,000 m over a width of more than 150 km, in contrast to the more southerly elements of the IBM arc. A seismic survey of the Izu arc was acquired in 1992, and this survey is historically important, because of the first inference of a laterally extensive mid-crustal layer with a P wave velocity of 6.1–6.3 km s^{-1}, which was interpreted to be granitic (Suyehiro et al. 1996). The wide-angle line across the Izu arc (Fig. 4.5) was recorded using 26 OBS spaced every 15–30 km, and shot using a 3-airgun 2,258 in^3 source, supplemented by 71 dynamite shots spaced every 2.5 km (Takahashi et al. 1998).

Further south, the Bonin arc has been subject to a more complex history of rifting than the Izu arc, and the seismic line across the arc, which was acquired in 2005, crosses the Eocene Ogasawara forearc ridge and two failed rifts, the Nishinoshima trough and the Ogasawara trough, located respectively west and east of the present-day volcanic line. The wide-angle seismic survey employed 110 OBS spaced every 5 km to record shots from an airgun array with total volume 12,000 in^3 (Takahashi et al. 2009). A 1,060 km-long profile was also acquired along the axis of the Izu-Bonin arc to show the along-strike variation in arc structure; shot in two phases this survey employed 103 OBS each time and the same 12,000 in^3 airgun array (Kodaira et al. 2007a, b).

Unlike the Izu-Bonin arc, the Mariana arc has undergone two episodes of rifting that developed to full back-arc spreading: initially in the Oligocene and later in the late Miocene. A seismic profile was acquired from the forearc, across the arc, the present-day back-arc spreading centre and the West Mariana ridge, which is the Miocene remnant arc. This line used 106 OBS spaced at 5–10 km intervals and an airgun array with total volume 12,000 in^3 (Takahashi et al. 2007, 2008). The Kyushu-Palau ridge, which is the older remnant arc, has a narrower expression in the seafloor bathymetry than the West Mariana ridge. The variation in crustal structure along the Kyushu-Palau ridge has been revealed by four profiles that were acquired across this remnant arc in 2004 using up to 200 OBS spaced at 5 km intervals, and a 8,040 in^3 airgun array (Nishizawa et al. 2007); two representative velocity models derived from this survey (Fig. 4.5) are included here. A 3D refraction survey, which involves an areal distribution of sources and receivers, has also been acquired over the central section of the Mariana arc (Calvert et al. 2008); 53 OBS were laid along three north–south lines and four north–south and seven east–west airgun lines were shot with a 10,810 in^3 airgun array.

4.5.3 Seismic Velocity Models

4.5.3.1 Cross-Arc Lines

The seismic velocity models across the arc are aligned at the trench and presented in Fig. 4.7 north to south with the Izu arc at the top. The two included seismic profiles from the Kyushu-Palau ridge lie at approximately the same latitude as the line across the Mariana arc and are shown on the left in Fig. 4.7, but these parts of the remnant arc actually originated further to the north, because the Parece Vela basin opened obliquely.

The crust of the Izu arc is inferred to be 18–21 km thick over at least 130 km of the east–west oriented

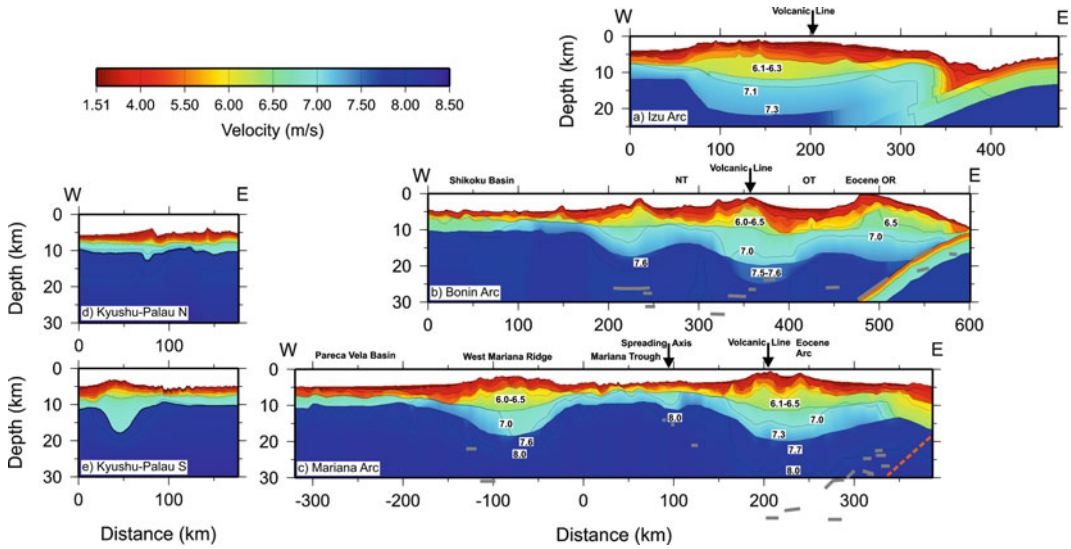

Fig. 4.7 Seismic velocity models across the Izu-Bonin-Mariana arc-back-arc system. (**a**) Line across the Izu arc (Suyehiro et al. 1996); (**b**) Line across the Bonin arc (Takahashi et al. 2009); (**c**) Line across the Mariana arc and remnant West Mariana ridge (Takahashi et al. 2007); (**d**) Northern line across the Kyushu-Palau ridge (Nishizawa et al. 2007); (**e**) Southern line across the Kyushu-Palau ridge (Nishizawa et al. 2007). The velocity models across the modern arc are aligned at the location of the trench. The lines across the Kyushu-Palau ridge are separated from the western end of the Mariana line by over 300 km of the Parece Vela basin, which is not shown here. The location of the top and bottom of the subducting oceanic crust beneath the Bonin forearc are constrained by wide-angle reflections. Beneath the Mariana forearc, the more steeply dipping oceanic crust is not resolved in this survey, but its approximate position is indicated by the *dashed orange line*. Grey line segments, some of which are at >30 km depth, indicate sub-Moho reflectors. Vertical exaggeration is 4:1.

profile (Fig. 4.7a), but the limited number of PmP reflections suggest that this thickness is not well constrained and the Moho is not identified at all under the forearc (Suyehiro et al. 1996; Takahashi et al. 1998). The midcrustal layer with velocities of 6.1–6.3 km s^{-1}, which reaches a maximum thickness of 7 km, also extends laterally over more than 100 km. This layer was introduced into the velocity model to reproduce the observed intracrustal reflections, and is also included, albeit in a less continuous form, in the velocity models across the Bonin and Mariana arcs. Although similar velocities are observed in the profile along-strike, the different tomographic approach used for inversion of the travel times of the strike line produces a velocity model with greater lateral heterogeneity (Fig. 4.4b), suggesting that greater compositional variation may be present in the middle crust of the Izu arc than implied by the first survey.

The velocity model across the Bonin arc shows the variation in crustal thickness caused by the two episodes of failed rifting here; the crust under the forearc Ogasawara ridge and the modern arc is as thick as 20 km, and the rear part of the arc reaches 15 km, but in the rift zones the crust thins to 9–12 km (Fig. 4.7b) with 2–3 km of this thickness comprising sedimentary rocks (Takahashi et al. 2009). The greater thicknesses of arc crust include mid-crustal regions with velocities of 6.0–6.5 km s^{-1} that are absent from the rift zones. In addition, Pn arrivals and some reflections from the upper mantle constrain velocities immediately below the inferred, laterally continuous (top)-Moho interface to be 7.5–7.6 km s^{-1}, leading to the interpretation of a crust-mantle transition zone up to 5 km thick beneath the thickest sections of arc crust. Under the rift zones, the Moho is inferred to be a sharp boundary.

In the Mariana arc, the initial Eocene arc lies 40 km east of the modern arc, but the crust, which is approximately 20–22 km thick (Takahashi et al. 2007; Calvert et al. 2008), does not appear to thin significantly between the two arcs (Figs. 4.1b and 4.7c) unlike the Bonin arc where the lateral separation due to rifting is greater at 150 km. However, the thickness of the mid-crustal

region with velocities of 6.1–6.5 km s^{-1}, is reduced by half between the Mariana modern and Eocene arcs. The crust of the 120 km-wide West Mariana ridge is up to 17 km thick, including a mid-crustal layer with velocities of 5.6–6.5 km s^{-1}. The smaller, 50 km-wide Kyushu-Palau ridge is 7–14 km thick (Fig. 4.7d, e), and lacks a significant region with velocities of 6.0–6.5 km s^{-1}, presumably due to its removal from the rear part of the arc massif. Velocities of 7.6–7.7 km s^{-1} inferred immediately below the top-Moho interface beneath the West Mariana ridge and the Mariana arc suggest crust–mantle transition zones are present beneath both the active arc and the remnant arc.

4.5.3.2 Along-Strike Variation

The velocity models obtained from the along-strike surveys reveal the variation in crustal structure of the Izu-Bonin arc from the collision zone with Japan in the north to the extended Bonin arc in the south (Kodaira et al. 2007b) (Fig. 4.4b). The seismic surveys were acquired along the modern volcanic line, and did not extend onto the failed rifts of the Bonin arc: the Nishi-noshima trough and the Ogasawara trough. Velocity models were derived independently using a multi-step procedure for each of the two ~500 km-long surveys, and then combined. In the first stage, a velocity model was derived using tomographic inversion of first arrivals, and this model was then locally updated to reproduce the arrival times of the wide-angle intracrustal reflections with these locations determined through migration of these second arrival picks (Kodaira et al. 2007a). This latter approach results in a model that lacks intracrustal interfaces that are continuous over large distances, e.g. more than 100 km, and variations in crustal velocity and thickness that occur over less than 50 km are quite apparent (Fig. 4.4b). The most striking feature of the velocity model, however, is the change in crustal thickness from 35 to 10 km, which is inferred from the 7.6 km s^{-1} velocity contour, and occurs over a distance of ~300 km. The thickness of the northern Izu arc is 26–35 km, but the Bonin arc is only 9–22 km thick. Lower average crustal velocities, more representative of an intermediate crustal composition, are inferred beneath the basaltic volcanoes of both the Izu and Bonin arcs, but higher velocities implying a more mafic crustal composition are found beneath rhyolitic arc volcanoes (Kodaira et al. 2007a).

4.5.3.3 3D Velocity Variation of the Mariana Arc

In contrast to 2D profiles, a 3D seismic survey can reveal the variation in seismic velocity throughout a subsurface volume, and the 3D velocity model obtained for the Mariana arc extends 240 km along strike (Calvert et al. 2008). Various crustal layer isopachs can thus be calculated from the thicknesses between iso-velocity contours. For example, an estimate of the igneous crustal thickness can be obtained from the depth interval between the 2.9 and 7.4 km s^{-1} contours (Fig. 4.8a). The igneous crust of the Eocene Mariana arc is thickest in the southern half of the main survey grid, reaching 22–24 km, and thins to 18–20 km further north. Along the modern arc, the crustal thickness reaches 20 km beneath most of the volcanoes, but decreases to approximately 16 km between them; this variation in crustal thickness is partly due to the inclusion of the volcanic edifices in the igneous crustal estimate. To the east of the Eocene arc, the forearc crust has a thickness of 13–16 km in the northern part of the survey grid, but the crust thins to 9–10 km in the south.

Isopachs of intermediate and mafic composition crust can be defined by the velocity ranges 6.0–6.5 km s^{-1} and 6.5–7.4 km s^{-1} respectively (Fig. 4.8b, c). Disregarding structures extending less than 20 km along strike, which are probably beyond the limit of resolution of the 3D tomographic inversion, the thickness of intermediate crust varies between 2 and 5 km along the modern arc, and only reaches a significant thickness near Sarigan, where three volcanoes have merged into a larger structure. Along the Eocene arc, intermediate composition crust is better developed, but it is not of uniform thickness along strike, varying between 3 and 6 km. Along the modern arc, the thickness of the mafic lower crust exceeds 12 km near the volcanic centers, but thins to 5–9 km between them, consistent with the inference that the modern arc is built on arc crust thinned by rifting (Oakley et al. 2009). Although thicker along the Eocene arc, the mafic lower crust thins from 15–18 km in the southern part of the survey grid to 12–15 km in the north. Along the modern arc, many of the thickness contours define approximately

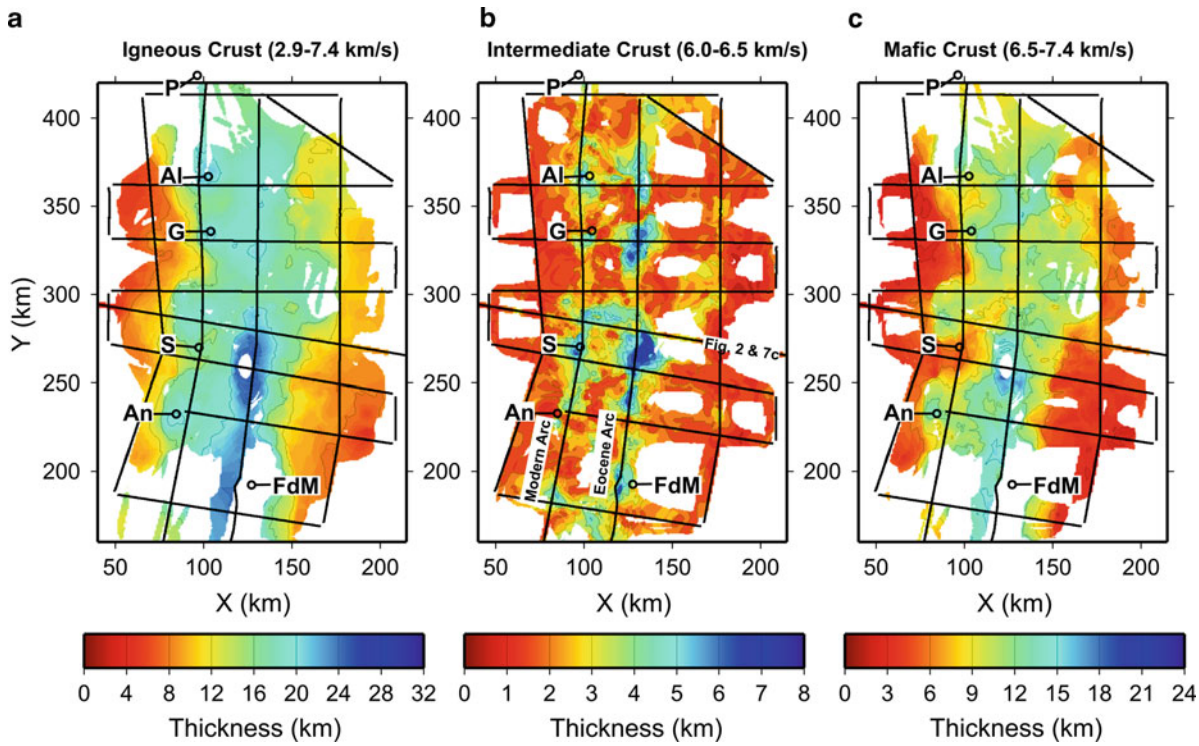

Fig. 4.8 Isopachs calculated from 3D tomographic velocity model: (**a**) Igneous crust (2.9–7.4 km s^{-1}); (**b**) Middle crust (6.0–6.5 km s^{-1}); (**c**) Lower crust (6.5–7.4 km s^{-1}). Note that the color-scale for the isopach thicknesses varies between different parts of this figure. P, Al, G, S, and An are the active volcanic islands of Pagan, Alamagan, Guguan, Sarigan and Anatahan. FdM is Ferdinand de Medinilla on the Eocene arc.

circular features, for example near Alamagan, Sarigan, and Anatahan, indicating focused crustal accretion over the last 4 Ma. In contrast, the contours beneath the Eocene arc are subparallel to strike, implying that these variations tend to even out over a longer period.

4.6 Lesser Antilles Arc

4.6.1 Tectonic History

The present arcs in the Caribbean region comprise a Great Caribbean island arc system that was originally formed in the Pacific Ocean, but migrated into the Atlantic Ocean as the Caribbean plate moved eastward (Burke 1988). At ~55 Ma, the Caribbean plate began to collide with South America in northwest Venezuela, resulting in the termination of subduction and volcanism in the Leeward Antilles arc (Fig. 4.9) as the collision migrated eastward. The Lesser Antilles arc initiated 12–15 Ma ago, and is separated from the Aves Ridge by the Grenada basin, which is believed to be underlain by oceanic crust (Boynton et al. 1979). The Aves Ridge is an extinct or remnant island arc that was originally active between ~90–55 Ma ago, and thus cannot be a remnant arc associated with the modern Lesser Antilles arc. The Grenada basin may have formed through back-arc spreading, e.g. Bouysse (1988), or, alternatively, the basin may have been created when an eastward jump in subduction trapped a piece of oceanic or forearc crust (Malfait and Dinkelman 1972). The Tobago and Grenada basins might originally have been continuous and only become separated with the more recent growth of the Lesser Antilles arc (Speed and Walker 1991);

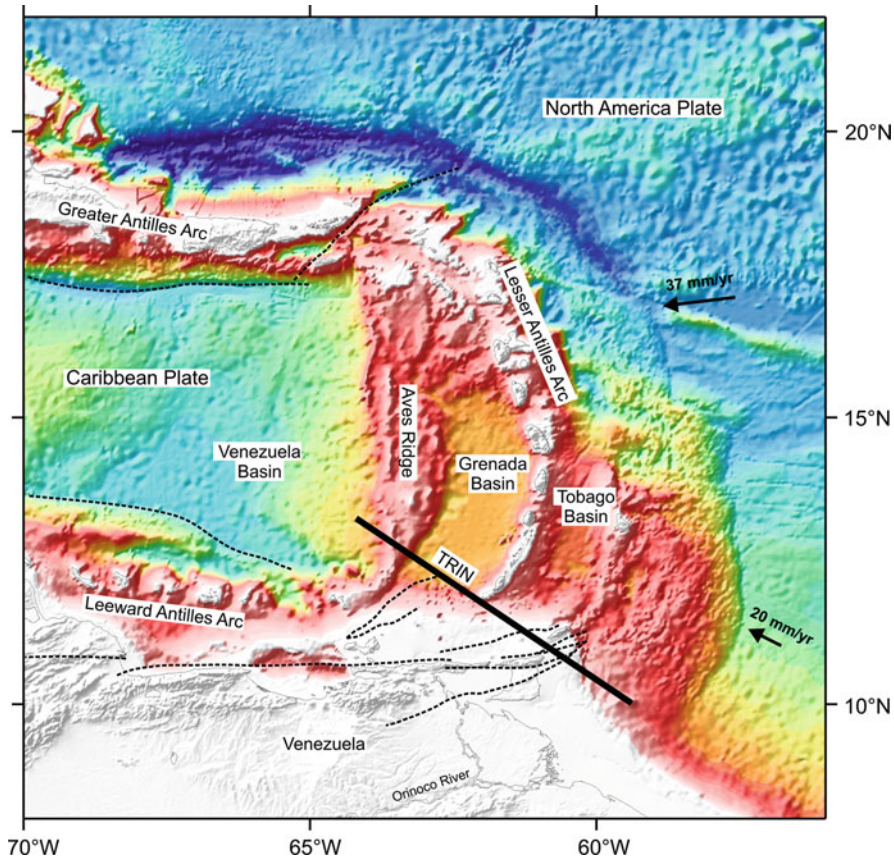

Fig. 4.9 Bathymetry of Lesser Antilles arc with the location of the TRIN seismic line. *Dashed black lines* indicate faults [after Christeson et al. (2008)]. The trench is well defined along the northern section of the arc, but further south the trench is obscured by the accretionary wedge that has evolved due to the high sediment input from the South American continent. The Aves ridge is interpreted to be a remnant arc that may have been active until ~55 Ma (Bouysse 1988). Seafloor depth scale is the same as in Fig. 4.2.

however, the complex nature of the Caribbean arc system means that many aspects of its evolution are still not well understood.

4.6.2 Seismic Survey and Velocity Model

A seismic survey, which employed 39 OBS spaced at 11–16 km intervals and an airgun source with volume 6,947 in^3, was acquired across the southern section of the Lesser Antilles arc (Fig. 4.9) in 2004 (Christeson et al. 2008). The crust of the active arc is approximately 24 km thick, and the crust of the remnant arc, the Aves ridge, is 26 km thick (Fig. 4.10). PmP reflections were recorded beneath the Aves ridge, Grenada basin and Tobago basin, but a Moho reflector appears to be absent beneath the active arc. In the back-arc basin and forearc of the Lesser Antilles arc, the top of the igneous crust probably lies close to the 4.5–5.0 km s^{-1} isovelocity contours due to its age and burial. Thus the back-arc and forearc basins are filled with a sedimentary section that is up to 12 km thick and overlies 4–10 km of igneous crust (Christeson et al. 2008). In general, the forearc region and back-arc basin of an island arc system represent a significant accommodation space that will rapidly fill if there is a high sediment input as is the case where the Lesser Antilles arc is close to the Orinoco river of South America.

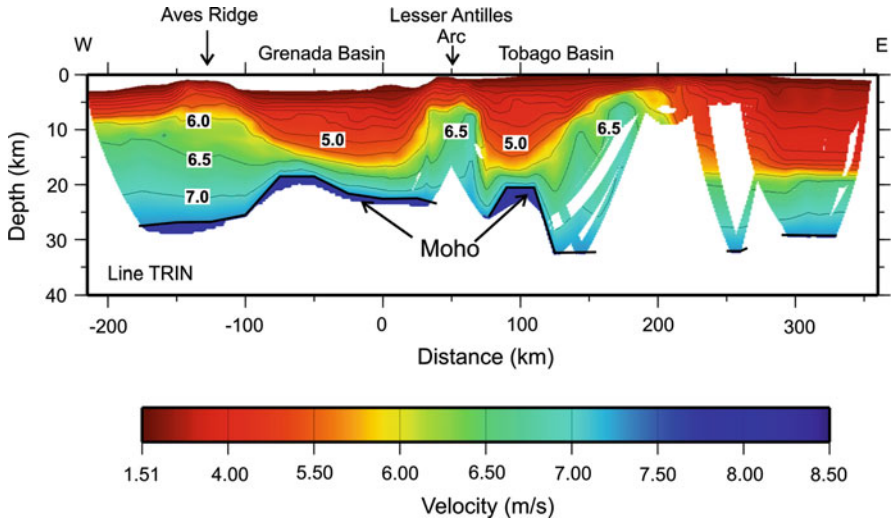

Fig. 4.10 Seismic velocity model across the southern section of the Lesser Antilles arc–continent collision zone (Christeson 2008). The base of the crust is primarily defined by PmP reflections from the Moho, which is shown by a *heavier black line* where constrained. The velocity model is not well-defined east of the Tobago basin due to the low ray coverage.

4.7 Deep Seismic Reflectivity Beneath Island Arcs

4.7.1 Wide-Angle Reflections

Wide-angle surveys of island arcs record reflections from within arc crust, the crust–mantle-transition and the uppermost mantle. These reflections are routinely incorporated into the derivation of the velocity models (see Sect. 3.1), but reflectors within the mantle wedge are somewhat surprising since they are not commonly observed in other tectonic environments. Deep reflectors beneath the Mariana and Bonin arcs, which have been located using migration of travel time picks, are shown in Fig. 4.7b, c. Since the migration of relatively sparse data can generate artifacts, the steeply dipping limbs have been excluded, and the reflectors are mostly shown as subhorizontal. Within the Mariana arc-back-arc system, reflectors occur in the uppermost mantle beneath the forearc, active arc, rear arc and remnant arc, with depths varying between 20 and 42 km (Takahashi et al. 2008). In the case of the Bonin arc, intra-mantle reflectors occur similarly across the arc system at depths of 22–32 km, and reflections are also recorded from the top of the subducting slab (Takahashi et al. 2009).

Although some mantle reflectors in the vicinity of the active arc could be attributable to melt, the existence of such reflectors beneath the remnant West Mariana ridge suggests that they are produced during the generation of island arc crust, frozen into the uppermost mantle and preserved by arc-rifting. Inferred velocity contrasts across the mantle reflectors are 7.6–7.9 km s^{-1} beneath the active Bonin arc (Takahashi et al. 2009) and perhaps as large as ~7.6–8.3 km s^{-1} beneath the Mariana arc (Takahashi et al. 2008).

4.7.2 Normal-Incidence Reflections

In principle, normal-incidence multichannel seismic reflection surveys can map laterally varying structures in the sub-surface with much greater resolution than more sparsely sampled wide-angle surveys. However, the interpretation of normal-incidence reflection data across island arcs is very challenging, because complex long-period water-layer multiples are generated by the deep variable seafloor, and high-amplitude coherent noise is produced by scattering from the rugose bathymetry around the seismic line. To illustrate the potential of this methodology, two unmigrated seismic sections are presented from areas

where the seafloor is relatively shallow; in such areas, water-layer multiples will decay more rapidly with recording time, and reflections from the lower crust and Moho can be more easily identified.

As with most island arcs, the seafloor depth of the IBM arc system is almost everywhere greater than ~200 m; however, shallow seafloor exists around the island of Farallon de Medinilla on the Eocene part of the Mariana arc. The hard seafloor produces a sequence of high amplitude multiple reflections in the data, but these have largely dissipated by a recording time of ~8 s (Fig. 4.11). Coherent dipping linear arrivals due to scattering around the seismic line (Larner et al. 1983) are also present. Nevertheless beneath the shallow seafloor, sub-horizontal low frequency reflections can be identified between 8 and 11.5 s in a 15-fold stack processed from the airgun shooting line from the 3D survey shown in Sect. 5.3.3. The 7.4 km s^{-1} isovelocity contour, which was interpreted to be the top of the crust–mantle transition zone in a coincident wide-angle seismic survey (Calvert et al. 2008), occurs at a depth of ~24 km here, corresponding to 9.0–9.5 s. The existence of reflections up to 2 s below this contour suggests that the crust–mantle transition extends down to ~32 km, if the downward termination of seismic reflections marks the top of the upper mantle.

The Aleutian arc differs from other intraoceanic arcs in that the seafloor is <200 m along most of the arc massif. Thus imaging of reflections from the deeper crust and upper mantle is not strongly affected by interfering water layer multiples. In fact high amplitude reflections from the top of the subducting Pacific plate visible in a 40-fold stack from line A2 (Fig. 4.2) demonstrate good signal penetration through the arc crust and mantle wedge (Fig. 4.12). These reflections from the top of the plate originate up-dip, i.e., out of the plane of this section. At the west end of the section, the downward termination of lower crustal reflections correlates closely with the position of the Moho inferred by Shillington et al. (2004), but further east the deepest identifiable lower crustal reflections, which are somewhat lower in amplitude, are ~2 s shallower than the Moho.

Despite seismic imaging difficulties, the lack of reported reflections from the igneous crust of island arcs suggests that arc crust is not strongly reflective. Yet the reflection data presented here show that lower crustal reflectors with an apparent lateral continuity of <10 km in unmigrated data can exist beneath island

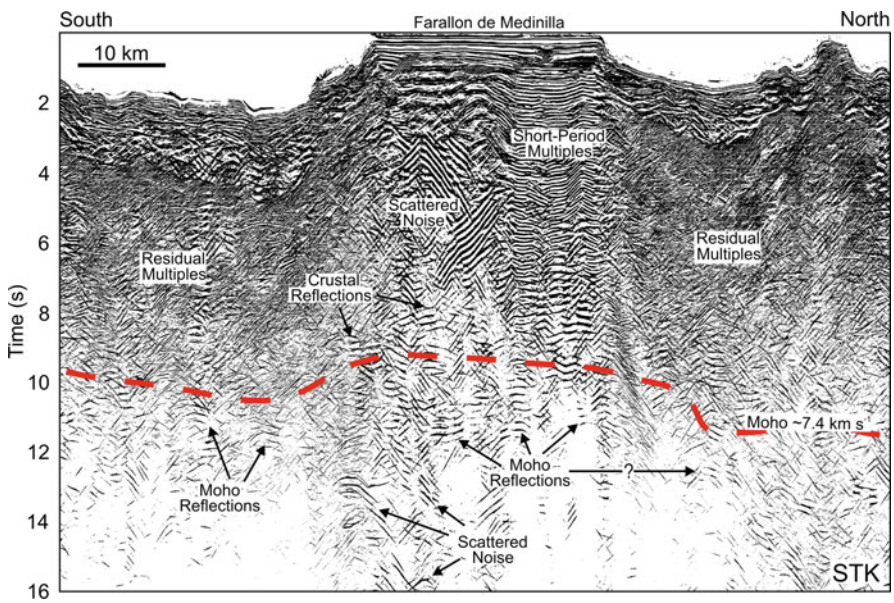

Fig. 4.11 Seismic reflection section along the inactive Eocene section of the Mariana arc. Low frequency reflections, which are laterally continuous over 4–8 km, can be identified between 8 and 11.5 s beneath the shallow seafloor around the island of Farallon de Medinilla. At earlier times, the section is dominated by interfering coherent noise. Reflections up to 2 s below the 7.4 km s^{-1} isovelocity contour, which was interpreted to represent the top of the crust–mantle transition in a coincident wide-angle seismic survey (Calvert et al. 2008), indicate that this transition zone may be ~8 km thick here.

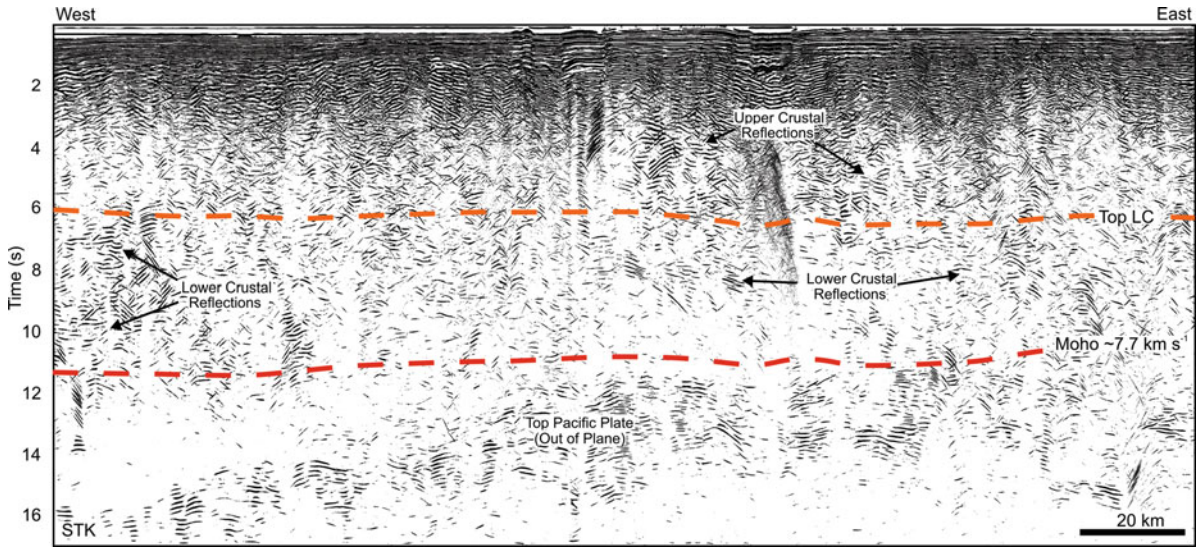

Fig. 4.12 Seismic reflection section along the Aleutian arc. Lower crustal reflections can be identified between 6 and 11 s at the western part of the section and between 6 and 8.5 s further east. Clear reflections from the top of the subducting Pacific plate indicate good signal penetration through the arc crust, but the top of the plate is deeper than it appears in this section, because these reflections originate up dip and out of the plane of this image. The times of the Moho and the top of the lower crust are derived from the velocity model of Shillington et al. (2004).

arcs. In extended arcs, some reflections in the igneous crust might indicate faults or shear zones, but in many cases the characteristics of these deep reflections, or their absence, are likely attributable to magmatic processes, and reflection surveys have the potential to constrain their lateral variability.

4.8 Interpretation of Seismic Velocity Models

The seismic velocities of rocks are affected by a number of factors, including mineralogy, porosity, pore fluid, temperature and confining pressure. In the interpretations of seismic velocity models from island arcs, porosity is considered to be a significant effect mainly in the upper crust, where volcaniclastic sediments and talus from the volcanic edifices can serve to reduce seismic velocities in the upper few kilometres; in the middle and lower crust, porosities are very low although seismic velocities can be affected if certain crack geometries are widespread (Hyndman and Shearer 1989). No localized velocity anomalies that could be interpreted as magma bodies have been inferred in any of the velocity models shown here, implying that the dimensions of any melt zone must be less than the limit of resolution of seismic refraction surveys. Given the magmatism associated with island arcs, it is likely, however, that there are significant lateral variations in temperature within the crust, which could extend over several tens of kilometers. The P wave velocities of igneous crustal rocks decrease with increasing temperature (Birch 1943; Kern 1978; Christensen 1979), and, in the absence of melting, a reduction in lower crustal velocity of 0.12 km s^{-1} has been suggested for the Aleutian arc relative to the same depth in the forearc region (Fliedner and Klemperer 1999). The thermal structure of most island arcs is not well known, but a similar difference in velocities is predicted at a depth of 20 km if the geothermal gradient varies from a high value of 40°C km^{-1} in the active arc to 25°C km^{-1} in the forearc. Given the relatively small effect of temperature on the magnitude of seismic velocity variation at a given depth, most authors interpret velocity variations inferred in the middle and lower crust in terms of mineral composition related to the volcanic arc's magmatic evolution. Such interpretations can be better constrained by a comparison of seismic velocity

models with laboratory measurements of velocity on samples from exhumed island arc crust or continental areas with similar lithologies.

4.8.1 Constraints from Laboratory Measurements

1D velocity-depth profiles were obtained for eight island arcs by laterally averaging the best constrained parts of their respective 2D seismic velocity models (Table 1), and then converted from depth to lithostatic pressure using an empirical relation between velocity and density (Brocher 2005). All profiles were also corrected to a common temperature of 25°C using a conservative geothermal gradient of 25°C km^{-1} and a thermal coefficient of -0.4 m s^{-1}°C^{-1}, which is consistent with a broad range of crustal rocks (Rudnick and Fountain 1995) and produces an increase in the observed velocities of 0.2 km s^{-1} at a depth of 20 km. These corrected 1D seismic velocity profiles are compared to the velocity variation with confining pressure of a number of representative lithologies from two regions where island arc crust has been exhumed: the Tanzawa plutonic complex (Nitsuma 1989) on the Japanese island of Honshu (TPC in Fig. 4.5) and the Kohistan-Ladkh terrane (Bard et al. 1980) of northern Pakistan and northwestern India (Fig. 4.13). Some average velocity functions, e.g. from the Tonga and South Sandwich arcs, only extend as far as the middle crust while others extend into to the uppermost mantle, e.g. the Mariana arc. The envelope of all velocity functions, which is shaded grey is relatively broad at pressures above 0.5 GPa, because the thickness of the crust varies from arc to arc.

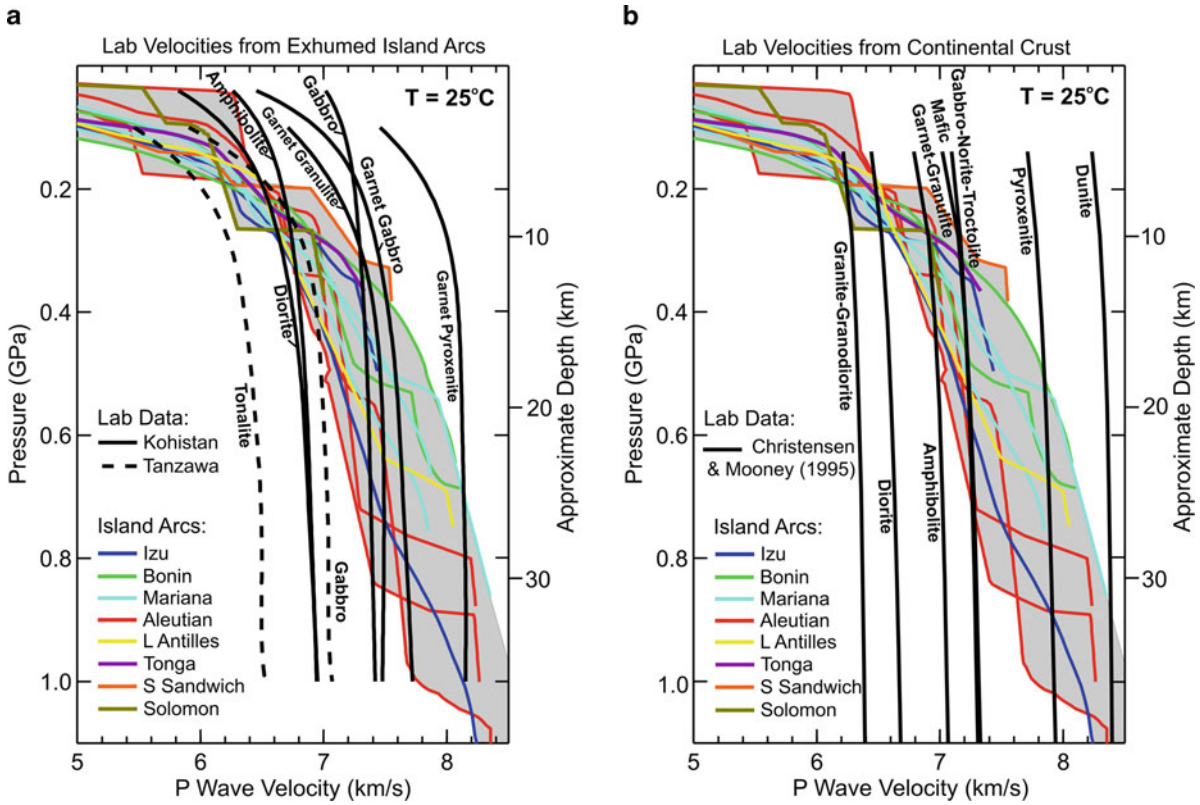

Fig. 4.13 Comparison of island arc velocity functions with laboratory measurements of P wave velocity in cores from: (**a**) Exhumed sections of island arcs; (**b**) Continental crust. The arc velocity profiles were obtained by averaging laterally the best constrained parts of the 2D velocity models, followed by conversion to confining pressure and correction to a constant temperature of 25°C using a thermal coefficient of -0.4 m s^{-1}°C consistent with most igneous rocks (Rudnick and Fountain 1995). The *shaded grey area* represents the range of velocities inferred in island arcs from wide-angle seismic surveys. The sources for the arc velocity profiles are listed in Fig. 4.14.

As pointed out by Behn and Keleman (2003), it is impractical to invert P wave velocity data for whole rock geochemistry, or to even determine in detail the SiO_2 content of igneous rocks; however, the comparison of seismic refraction models with measurements on core samples data and velocities calculated for given compositions can guide a first order interpretation.

The suite of tonalitic and gabbroic plutons of the Tanzawa plutonic complex was exhumed in the collision between the northernmost Izu arc and the Honshu arc that began ~7 Ma ago (Kawate and Arima 1998; Yamamoto and Kawakami 2005). These plutons intruded volcanic rocks, hemipelagic sediments, and volcaniclastic sediments of the Miocene Tanzawa Group whose metamorphism indicates a maximum depth of approximately 6 km (Arai 1987). Once thought to be the middle crust of the Izu arc, recent U-Pb geochronology has shown that while one tonalite has an age of 9 Ma, the others are approximately 4–5 Ma old and thus syncollisional (Tani et al. 2010). Measurements of P wave velocity versus confining pressure for three tonalites (56–71% SiO_2) and three gabbros (43–54% SiO_2) (Kitamura et al. 2003) were each averaged and fit with a fifth-order polynomial to create a lithology-specific velocity variation (dashed lines in Fig. 4.13a).

The exposed Cretaceous Kohistan arc was obducted during the collision of India with Eurasia, and comprises a near-complete crustal section extending from upper crustal volcanics to the uppermost mantle. The arc initially developed in an intra-oceanic setting, but formed an Andean-style margin after its accretion to Euriasia (Burg in Chap. 10; DeBari et al., in Chap. 5). Using velocity measurements published by Miller and Christensen (1994), representative velocity variations with pressure have been calculated for diorite (44–76% SiO_2), amphibolite (47–57% SiO_2), gabbro (43–50% SiO_2) and garnet gabbro (41–52% SiO_2 with 30–50% garnet) and these data are shown with solid lines in Fig. 4.13a. Lab measurements from Kono et al. (2009) have been used to derive velocity variations for garnet granulite (49–52% SiO_2 with 24–37% garnet) and garnet pyroxenite (41–48% SiO_2 with 15–60% garnet); the garnet granulites of Kono et al. (2009) are similar rocks to the garnet gabbros of Miller and Christensen (1994).

At low confining pressures, the laboratory P wave velocities increase notably with increasing pressure due to the closure of microcracks in the sample (Kitamura et al. 2003), but at pressures greater than ~0.5 GPa, the velocity variation with pressure is considerably less, and the difference in velocity of the various lithologies is related to their different (to first order mafic) mineral content. A similar relationship is seen with velocity measurements on lithologies from a broad range of continental crust (Fig. 4.13b). The velocity variation within specific lithologies at a given confining pressure is indicated by standard deviations from Christensen and Mooney (1995), which typically range from ~0.1–0.25 km s^{-1}, with gabbro-norite-troctolite being at the upper end of this range. Gabbros from the Kohistan arc have higher velocities than those from the Tanzawa plutonic complex, consistent with this finding.

At pressures greater than 0.2 GPa, the tonalites from the Tanzawa plutonic complex exhibit lower velocities than those found in any island arc, even allowing for a reasonable velocity variation between different samples. This observation indicates that voluminous tonalite is only likely to occur in island arcs at depths less than ~8 km. The relatively high velocities in the upper crust of the Aleutian arc suggest the presence of significantly more mafic rocks. Although the geothermal gradient and thermal coefficient introduce some uncertainty, island arc velocity profiles derived from seismic refraction surveys are consistent with a composition somewhere between diorite and gabbro at pressures of 0.2–0.3 GPa. At greater pressures, seismic velocities correspond to gabbroic rocks with a lower quartz content. Temperature-corrected P wave velocities greater than approximately 7.4 km s^{-1} may indicate the presence of garnet in gabbros with a low plagioclase content or pyroxenites characteristic of restites (Kitamura et al. 2003).

4.8.2 Upper Arc Crust

In general, the upper crust of island arcs can be viewed as a layer of sedimentary rocks derived through a range of processes overlying igneous crust, but in detail the uppermost crust is commonly heterogenous due to volcanism and intrusion into the upper crustal section, as demonstrated in the Tanzawa plutonic complex. In many arc velocity models, an uppermost, relatively low velocity sedimentary layer has been defined using coincident multichannel seismic reflection data, stacking velocities and/or velocities from first arrival tomography of the towed streamer data. These sediments

accumulated in small basins within the arc massif, on the flanks of the arc itself or in the deep ocean basin. The base of this layer is typically defined by a sharp increase in velocity in the models, and may directly overlie the igneous crust, for example as interpreted along the strike of the Aleutian arc where the velocities beneath the sedimentary layer are 6.0–6.5 km s^{-1}. In other arcs, the increase in velocity at the base of the upper sedimentary layer is smaller, but a high velocity gradient exists in the underlying layer, with velocities increasing downward from ~3.5 km s^{-1} to >5.0 km s^{-1} over a few kilometers. Such a region may correspond to interbedded, and variably metamorphosed volcanics, hemipelagic and volcaniclastic sediments intruded by plutons of different ages and composition.

At shallow depths, basaltic rocks can have relatively low velocities, making them difficult to identify on the basis of P wave velocity alone. For example, velocities as low as 2.5–3.0 km s^{-1} have been inferred in the extrusive basaltic layer of 0–3 Ma old oceanic crust using OBS surveys, and a gradual increase in velocity to 3.5–4.5 km s^{-1} by 4–5 Ma, and to 4.0–5.5 km s^{-1} at ages greater than 50 Ma due to porosity reduction has been documented (White 1984). In island arcs, the increase in velocity with depth may be partly associated with a comparable reduction in porosity through compaction and the filling of pores by hydrothermal circulation, and an increasing prevalence of intrusive rocks. The base of the upper crust has been interpreted in most arc velocity models to be located where the high velocity gradient, which is characteristic of the upper crust, decreases sharply and the P wave velocity reaches approximately 6.0 km s^{-1}, but this value is 6.5 km s^{-1} in the case of the line along the Aleutian arc. This strike line suggests that the upper crust of the Aleutian arc is largely basaltic, because the velocities are 6.0–6.5 km s^{-1} at depths as shallow as 2 km where fracture porosity reduces P wave velocity values. At such shallow depths, felsic rocks would likely have velocities below 6.0 km s^{-1}, but the unknown porosity is a source of significant uncertainty.

4.8.3 Middle Arc Crust

The middle crust has been defined in different studies both in terms of seismic velocity and as the region between intracrustal reflectors with some degree of lateral continuity along a seismic profile. In surveys across the IBM arc system, for example, the mid-crust is interpreted to be the region with velocities between 6.0 and 6.5 km s^{-1} between two intracrustal reflectors, e.g. Takahashi et al. (2007). Kodaira et al. (2007a) refer to the region with these velocities as the upper middle crust and a deeper region with velocities of 6.5–6.8 km s^{-1} as the lower middle crust; however, Takahashi et al. (2007) and Calvert et al. (2008) associated velocities of 6.5–6.8 km s^{-1} with the upper part of the lower crust. In the Aleutian arc, which is generally characterized by higher seismic velocities, the mid-crustal layer has velocities of 6.5–7.3 km s^{-1} with the upper and lower boundaries constrained by intracrustal reflections. With the greater thickness of Aleutian arc crust, the base of the middle crust occurs here at a depth of 15–20 km, and it is worth noting that these depths correspond to the lower crust along much of the IBM arc, and even the upper mantle in those parts of the Bonin arc where the crust has been thinned by rifting. Thus the term middle crust is not used in a way that is consistent between surveys, in part due to the different approaches to analysis of the various seismic surveys, but also due to the term's implicit relation to overall crustal thickness. Here I shall assume that arc crust can be loosely divided into upper, middle and lower regions with approximate relative proportions of 3, 4, and 5 respectively, and the term middle crust will be used loosely to refer to that third of the crust between the upper and lower regions. Where a region predominantly within the middle crust is bounded by two intracrustal reflectors, the term mid-crustal layer, which allows a broad range of seismic velocities within it, will be used. Inferred crustal composition is better associated with regions characterized by a specific range of seismic velocities (but with the implicit assumption of a depth range, i.e., confining pressure) than a generalised "middle crust".

Based on seismic velocity measurements on samples from the Tanzawa plutonic complex, velocities of 6.0–6.5 km s^{-1}, which are too low to be most gabbroic rocks at depths of 5–15 km, indicate the presence of tonalitic rocks, but the higher end of this velocity range is too high to be consistent with pure tonalite. Mapping of the Tanzawa plutonic complex suggests that the middle to upper crust of the Izu arc includes plutonic rocks that range from pyroxene-hornblende gabbronorite to relatively quartz rich tonalite (Kawate and Arima 1998). It is an oversimplification to

associate a single lithology with velocities of 6.0–6.5 km s^{-1}, which probably represent a region of average "intermediate" composition similar to quartz gabbro that comprises tonalite, diorite and gabbro. Within the IBM arc, the thickness of the region in the upper and middle crust with velocities of 6.0–6.5 km s^{-1} varies between 2 and 8 km. Such seismic velocities are only found in the uppermost crust of the Aleutian arc.

P wave velocities of 6.5–6.8 km s^{-1} indicate a crust more dominated by gabbroic lithologies. Velocities lower than 6.9 km s^{-1} are difficult to simulate in pristine gabbros using models of mantle melting (Korenaga et al. 2002), but the velocities of gabbroic rocks recovered from ocean crust by drilling are 6.5–7.4 km s^{-1} (Iturrino et al. 1991; Iturrino et al. 1996). These lowest velocities in oceanic crust may arise from ridge-crest faulting and thermal contraction (Korenaga et al. 2002). Faulting associated, for example, with arc rifting in the IBM arc-back-arc system or block rotation in the Aleutian arc could locally reduce gabbroic velocities in island arcs. It is also possible that velocities of 6.5–6.8 km s^{-1} indicate a region comprising plutons of both gabbroic and intermediate composition with a reduction in the volume of intermediate composition rocks with increasing depth and seismic velocity. The rugose velocity contours shown in some of the velocity models, e.g. along the Izu-Bonin arc could be an indication of this heterogeneity. There is also a large range of velocities, 6.5–7.3 km s^{-1}, within the mid-crustal layer of the Aleutian arc, but the average velocity of 6.92 km s^{-1} indicates a primarily gabbroic composition with lower velocities perhaps associated with the local presence of more felsic rocks (Shillington et al. 2004).

4.8.4 Lower Arc Crust

In many surveys of arc crust, the Moho is usually located using PmP reflections, because few Pn diving waves are observed at offsets >120 km. The lower crust is commonly bounded below by this reflector. Seismic velocities in the lower crustal layers beneath the Izu, Bonin and Mariana arcs are 6.8–7.3 km s^{-1}, 6.7–7.4 km s^{-1}, and 6.8–7.4 km s^{-1} respectively. In the lines across the Aleutian arc, velocities of 6.9–7.2 km s^{-1} were inferred in this layer along line A1 in the west and 6.9–7.5 km s^{-1} along line A3 in the east; velocities of 6.8–6.9 km s^{-1} at the northernmost end of line A3 could indicate the presence of continental crust associated with the former Beringian margin. As discussed above, these velocities are essentially consistent with the presence of quartz-poor gabbroic plutons; however, velocities as high as 7.4–7.5 km s^{-1} may indicate either ultramafic cumulates or perhaps partially intruded, partially serpentinized peridotite as suggested beneath the forearc of line A3 (Lizarralde et al. 2002). Lower crustal velocities of 7.3–7.7 km s^{-1} derived along the strike of the Aleutian arc are higher than found on the intersecting profiles, but the interpretation of a mixture of mafic and ultramafic rocks, including garnet-bearing assemblages, is generally similar (Shillington et al. 2004). Along line A2, higher velocities occur at the centre of a structural block, leading Shillington et al. (2004) to suggest that lower temperatures here result in relatively high pressure fractionation and a greater volume of mafic restite.

4.8.5 Crust–Mantle (Moho) Transition Zone

The thickness of arc crust is often constrained by PmP reflections, but where large offset Pn arrivals are well recorded velocities immediately beneath the Moho reflector have been found to be significantly lower than typical upper mantle velocities; velocities of 7.7 and 7.6 km s^{-1} were found below the Mariana arc and remnant West Mariana ridge respectively (Takahashi et al. 2007). An upper mantle velocity of 7.8 km s^{-1} is only attained 4 and 3 km below the Moho reflector respectively, suggesting the presence of a vertically distributed crust–mantle transition. Although the presence of melts or serpentinized mantle peridotites might explain low velocities under the modern arc, neither explanation is likely to apply beneath the remnant arc where there is no water rising from the subducting slab. It seems more plausible that a gradual crust–mantle transition zone is a primary feature of island arc formation.

Kodaira et al. (2007a) similarly interpret a 5–10 km thick layer with velocities of 7.2–7.6 km s^{-1} at the base of the Izu-Bonin arc crust. Sato et al. (2009) modelled the elastic response of wide-angle reflections from the top and bottom of the Izu crust–mantle transition, and

estimated that the P wave velocity contrasts varied from approximately 0.2–0.4 km s^{-1} along the arc; where the contrast at the top of the layer was high, the contrast at the base was relatively low, and vice versa. If the uppermost mantle comprises olivine cumulates, i.e., dunite, formed during initiation of the arc, then the crust–mantle transition zone is probably a mixture of olivine cumulates and mafic restite (Tatsumi et al. 2008). The laterally varying velocity perturbations at the top and bottom of the crust–mantle transition could thus indicate the relative proportion of these two components; for example, a small upper velocity contrast over a larger lower contrast would indicate a lower proportion of olivine cumulate (Sato et al. 2009). In thicker arcs, pyroxenites may be more likely to occur at the crust–mantle transition than dunite (DeBari et al., in Chap. 5). This form of heterogeneity in the Mariana crust–mantle transition could generate the normal incidence seismic reflections tentatively identified over a depth range of ~24–32 km beneath Farallon de Medinilla in the Mariana arc (Fig. 4.11).

Most PmP reflections appear to originate from the top of the crust–mantle transition layer, and fewer wide-angle reflections are recorded from the base, e.g. Takahashi et al. (2009), perhaps because the contrast at the base of the crust–mantle transition is commonly smaller than at the top (Sato et al. 2009). Thus under an island arc, the interface that generates PmP reflections is best considered a top-Moho reflector, and the crustal thickness estimates quoted in this paper relate either to this reflector or a proxy for it, such as an isovelocity contour.

During repeated episodes of basaltic underplating, reaction of plagioclase with clinopyroxene can produce garnet in mafic restite if the depth is greater than approximately 25 km (Behn and Keleman 2006; Tatsumi et al. 2008), increasing the seismic velocity to 7.3–7.7 km s^{-1} (see also Fig. 4.13); however, the depth at which garnet occurs is quite sensitive to the geotherm. At depths greater than 30 km, garnet-producing reactions can also increase the seismic velocity of pyroxenites (Kono et al. 2009). Thus an alternative suggestion is that reflectors at the crust–mantle transition or within the uppermost mantle wedge might arise from a sudden downward increase in the proportion of garnet (Shillington et al. 2004; Takahashi et al. 2008). In the Kohistam paleo-arc, the crust–mantle transition is exposed as a continuous mafic-ultramafic layered intrusion progressing downward in paleodepth from garnet gabbro/garnet granulite, to garnet pyroxenite, to pyroxenite/dunite; the presence of garnet is due to the 36–45 km depth of the lowermost crust in a mature arc (Garrido et al. 2006). At the transition from garnet gabbro to garnet pyroxenite, the P wave velocity increases from 7.3–7.7 to 7.9–8.3 km s^{-1} due to disappearance of plagioclase which determines the base of the Moho transition zone in this setting (Kono et al. 2009). The presence of garnet will increase the average seismic velocity of the deep crust, but it is uncertain whether its distribution will cause seismic reflections. A crust–mantle transition zone is also observed in relatively thin arcs such as the Bonin arc; the 7.5 km s^{-1} contour lies at a depth of 15–20 km (Fig. 4.7b). In this shallower setting, the crust–mantle transition is likely to be a gradual change from mafic to ultramafic lithologies with minimal garnet present.

4.9 In Situ 1D Velocity-Depth Functions

Average in situ 1D velocity-depth functions have been obtained for several island arcs by laterally averaging sections of 2D velocity models derived by various authors (Table 4.1 in Appendix). The envelope of these velocity functions is shaded grey area in Fig. 4.14a. Line A3 across the Aleutian arc extends onto the continental crust of the Beringian margin, which is characterized by a mid-crustal layer of 6.4 km s^{-1} and a lower crust with velocities of 6.8–6.9 km s^{-1} (Fig. 4.2), and the proximity of this crust to the volcanic line is sufficient to perturb the average 1D velocity-depth function here into the range of continental profiles (dashed red line in Fig. 4.14a).

A seismic profile oriented along an island arc samples a greater volume of arc crust, and is thus likely to be more representative. The difference in the shape of the four 1D velocity functions along the IBM arc is primarily due to the variation in crustal thickness between the arcs (Fig. 4.14b). The Izu arc, which is well characterized by the recent survey of Kodaira et al. (2007a), is up to 35 km thick, and its average velocity profile in the middle and lower crust differs from that of the Aleutian arc by <0.3 km s^{-1}. In fact, the most striking difference between the Izu and Aleutian arcs is the presence of velocities of 6.0–6.5 km s^{-1} in the upper 5 km of the Aleutian arc, which is well

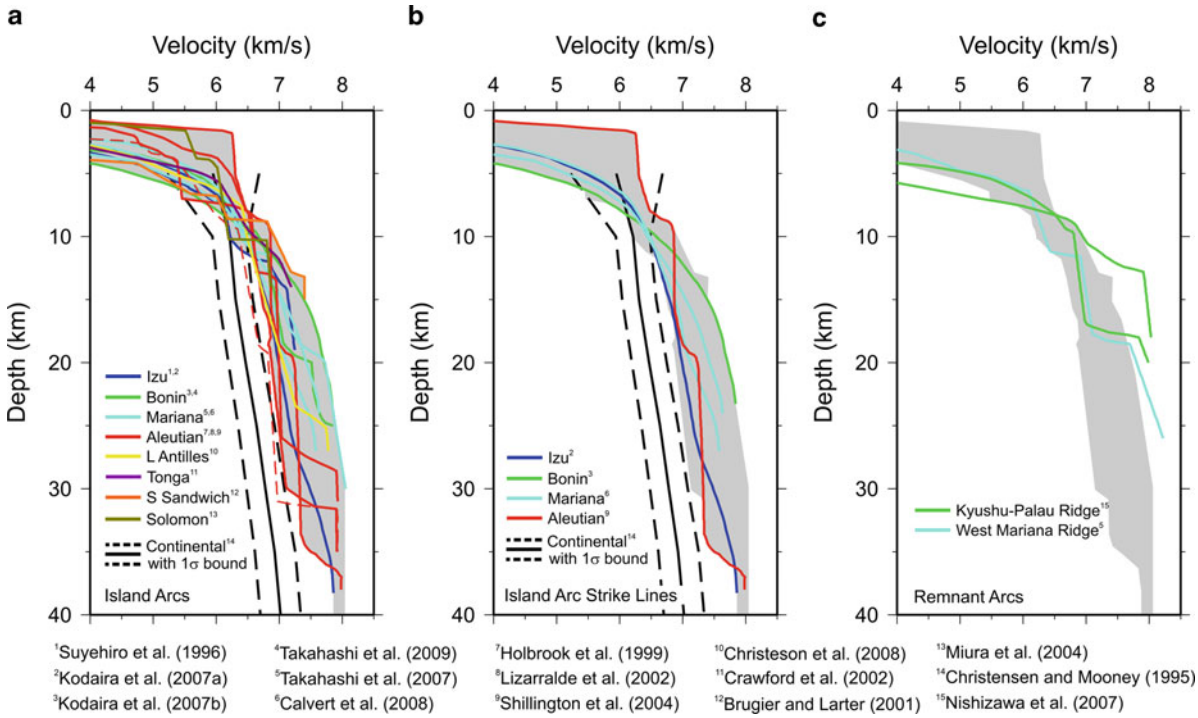

Fig. 4.14 Comparison of in situ island arc velocity profiles with the range of velocity values estimated for continental crust from wide-angle seismic surveys: (**a**) All island arc surveys; (**b**) Lines along island arcs, which represent a relatively large volume of arc crust; (**c**) Remnant arcs. The *grey shaded area* encompasses 1D velocity profiles from a broad range of island arcs. The *dashed red line* is derived from around the volcanic line on line A3 across the Aleutian arc, but the velocities in this profile are lowered by continental crust of the former Beringian margin.

constrained by streamer tomography (Shillington et al. 2004). These higher velocities may be attributable to the erosion of an original carapace of relatively high porosity flows and volcaniclastic rocks, resulting in an extensive, high velocity arc massif with a seafloor less than 200 m deep (Fig. 4.2), in contrast to the deep water settings of most other island arcs.

Remnant arcs tend to fall outside the envelope of functions for active island arcs due to their variable seafloor depth and crustal thickness, which are controlled by the original locus of arc rifting. For example, some crustal sections of the Kyushu-Palau ridge are only slightly thicker than oceanic crust (Fig. 4.7d), because rifting occurred in the rear arc.

The velocity depth functions used to represent continental crust in Fig. 4.14 were obtained after removal of the sedimentary basins (Christensen and Mooney 1995), and any comparison with island arc crust should, strictly speaking, use arc velocity functions referenced to the top of the igneous crust. Identification of the top of the igneous crust in island arcs is not straightforward due to the presence of high porosity volcanic rocks and intrusions within the shallow sedimentary section. Taking the 3.5 km s^{-1} isovelocity contour to be an approximation to this boundary, as is so at mid-ocean ridges (White 1984), a representative 1D velocity function for island arcs has been calculated using this datum (Fig. 4.15). (See Table 4.2 in Appendix for tabulation of reference velocity functions for this datum, as well as seafloor and mean sea level datums). Above a depth of ~8 km, island arc velocities are similar to those of continental crust and consistent with the presence of felsic rocks; however, seismic velocities in the uppermost crust can also be lowered by the increased porosity found there, and, as mentioned previously, the velocities in the uppermost crust are also consistent with porous mafic rocks. At depths greater than ~8 km, island arc crust is on average characterized by higher in situ seismic velocities, and is hence more mafic, than continental crust. Generation of continental crust directly from island arcs would require the removal of the large volume of crust that presently exists at depths greater than 10 km.

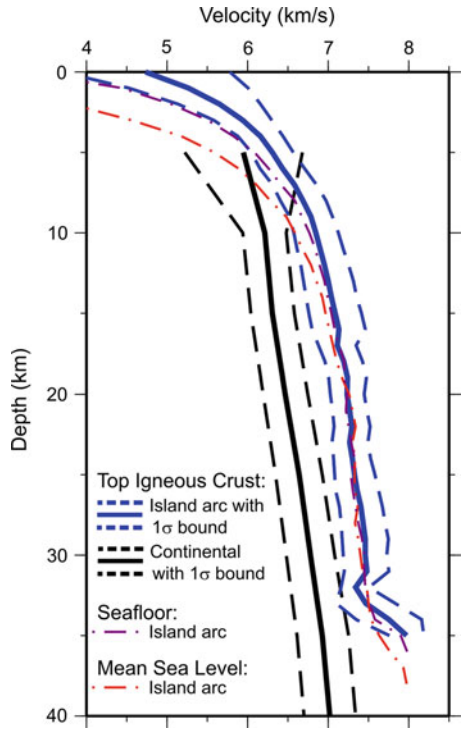

Fig. 4.15 Comparison of the average seismic velocity functions for island arcs with that of continental crust from Christensen and Mooney (1995). The different depth datum levels are indicated. Note that the range of data included in the island arc average decreases below 30 km depth, because there are few velocity models that extend this deep.

4.10 Evolution of Island Arc Crust

Although 1D velocity functions reveal the typical average velocity variation with depth in island arc crust, significant lateral variations can be present along strike; for example, the thickness of crust with velocities of 6.0–6.8 km s^{-1} increases beneath, or close to, basaltic volcanoes along the Izu arc, and decreases beneath rhyolitic volcanoes (Kodaira et al. 2007a). A variation in the thickness of crust with velocities of 6.0–7.0 km s^{-1} is also observed along the Eocene Mariana arc (Calvert et al. 2008), but as with the Izu arc, most of the lateral variation is associated with velocities greater than 6.5 km s^{-1}. Thicker regions of crust with velocities of 6.0–6.8 km s^{-1} have been interpreted to indicate locally elevated generation of tonalitic crust; however, at depths greater than 8 km the crust is intermediate to mafic in terms of its average bulk composition. Over the >40 Ma life of the IBM arc, repeated episodes of magmatic intrusion into the lower crust have resulted in anatexis and intracrustal differentiation; see, for example, Tatsumi et al. (2008) and DeBari et al., in Chap. 5. While intermediate composition magmas generated by this process rose into the upper crust, some of these magmas may have solidified at depths as great as 20 km, reducing the seismic velocities from those characteristic of quartz-poor gabbro.

Generation of intermediate composition magma by melting of basaltic crust will produce a residuum of pyroxenite restite (Nakajima and Arima 1998), implying an increase in the volume of high-velocity mafic rocks in the lower crust. However, thickening of the lower crust beneath thicker regions of inferred intermediate composition is not typically observed; in tomographic velocity models the mafic lower crust commonly becomes thinner (Calvert et al. 2008), as can be observed at 180 km, 250 km, 320 km in Fig. 4.4b in the case of the Izu arc. Two alternative explanations for the observed decrease in the thickness of the high velocity lower crust beneath regions of growth in intermediate crust are:

1. With an in situ P wave velocity of 7.3–7.6 km s^{-1} (Behn and Keleman 2006), pyroxenite restite can lie below the Moho in several velocity models, suggesting that the generation of intermediate composition melts can raise the level of the interpreted Moho, a seismologically defined boundary, within a petrologic lower crust and produce an apparent thinning of high velocity lower crust (Tatsumi et al. 2008).
2. With a density of 3.2–3.9 g cm^{-3} (Nakajima and Arima 1998), which is similar to or greater than peridotite in the uppermost mantle, restite may have detached from the arc crust and foundered. If this speculation is correct, then arc crust with a relatively thin high velocity lower crust could be an indication that this delamination process has occurred. In a detailed analysis of the stability of arc lower crust, Behn and Keleman (2006) show that pyroxenite and gabbronorite characteristic of arc lower crust can become denser than underlying harzburgite at pressures greater than ~0.85 GPa, i.e., ~30 km depth, due to the decrease in the amount of plagioclase and the formation of garnet in some rocks. Gravitational instability has thus been suggested if arc crust grows to more than 30 km thick; however, some island arcs, e.g. the Bonin arc, may not reach such thicknesses due to multiple episodes of extension that limit their vertical growth.

4.11 Comparison of Aleutian and IBM Arcs

In terms of seismic structure, the northern Izu arc, whose rear arc was subject to one episode of rifting in the Oligocene that created the relatively thin Kyushu-Palau ridge (Okino et al. 1994), appears most similar to the Aleutian arc with a somewhat less mafic composition, and a crustal thickness of 26–35 km versus the 35 km of the Aleutian arc. In contrast, the Bonin arc was subject to extension in the Eocene, which placed the Ogasawara Ridge in the forearc (Ishizuka et al. 2006), rifting of the rear arc in the Oligocene to remove the Kyushu-Palau ridge, and probably another episode of extension to create the Nishinoshima Trough, whose origin is poorly understood. As a result, the Bonin arc and forearc extend over 400 km from the trench, and comprise three distinct crustal blocks, none of which exceeds a thickness of 20 km, separated by thinned arc crust 10–12 km thick (Fig. 4.7b). The broad region of thin, 10–17 km thick, arc crust identified on the strike line (Fig. 4.4b) is likely a consequence of separation of the Ogasawara ridge, consistent with the suggestion that much of the arc crust was generated early in its history (Stern and Bloomer 1992). As indicated by the along-strike velocity profiles in Fig. 4.14b, the Mariana arc has a seismic structure intermediate between the northern Izu and Bonin arcs, which is presumably due to the Mariana arc massif being subject to less extension than the Bonin arc.

Arc rifting may result in the addition of high velocity magmatic material to the base of both the active and remnant arcs by decompression melting similar to that which has created magmatic underplates at some passive continental margins (Takahashi et al. 2008). In the case of the Mariana arc and West Mariana ridge, this characteristic mafic underplate appears to be a relatively small proportion (<5–8%) of the total crustal volume, but modification of arc crust by rifting is an issue that merits more detailed study.

Since the Eocene the average magmatic production rates of the Aleutian and Mariana arcs are estimated to be 82 km^3/km/Ma (Holbrook et al. 1999) and 80 km^3/km/Ma (Calvert et al. 2008) respectively, which fall within the range of 30–85 km^3/km/Ma derived for several arcs in the western Pacific (Dimalanta et al. 2002). Although these estimates of average productivities of the Aleutian and IBM arcs appear to be generally similar, differences in the distribution and volume of crust within these two arcs could be attributable to spatial and temporal variations in the magmatic flux from the mantle in addition to the effects of extension and arc rifting.

4.12 Implications for Arc–Continent Collision

Most island arcs, including both the Aleutian and IBM arcs, lie distant from continental areas and are subject to a restricted terrigenous sediment supply. As an island arc approaches a continental margin the sediment input to the arc will increase, very significantly in some cases due to uplift and erosion in the collision zone, and a thick sedimentary section can develop on the flanks of the island arc, across the forearc, and fill

the back-arc basin, if present. The Lesser Antilles arc is an example of this situation where sediment derived primarily from the northern margin of South America has formed a large accretionary wedge east of the Tobago basin, obscuring the trench in the southern part of the subduction zone (Fig. 4.9). Therefore prior to collision, the crust surrounding an island arc is likely to develop a much thicker sedimentary section due to this relatively late sedimentary input than implied by the tomographic velocity models from the Aleutian and IBM arcs, which now lie far from continental sediment sources.

Along-strike variations in the thickness of island arc crust, which ranges from 10–35 km in the case of the Izu-Bonin arc, will strongly influence the structural style of any arc–continent collision in which it is involved. Thin crust may be either obducted or underplated depending on its composition, and hence buoyancy, relative to a passive continental margin. Thick arc crust may be accreted to the edge of the incoming margin; for example, the 35 km-thick Stikinia arc terrane is interpreted to have partly overridden and accreted to the paleo-margin of western North America (Cook et al. 2004). The transition between these two processes might occur over distances along the strike of the arc as small as 300 km, the distance over which the Izu-Bonin arc thins from 35 to 10 km. Since the incoming arc will often be oblique to the margin this distance may be smaller along the strike of the collision zone. The seismic velocity variations inferred within the mid-crust of the Izu arc suggest that compositional variations at a scale of 50 km may also be apparent in accreted arc rocks.

Where a rifted island arc and its associated remnant arc are involved in arc–continent collision, the final post-collision geometry after closure of the ocean basin may contain a repetition of arc rocks with similar ages separated by younger arc rocks from the successor arc created after the initial collision, assuming that there has been not flip in subduction polarity.

4.13 Conclusions

A compilation of 1D seismic (P wave) velocity functions from eight island arcs, which are derived from well-constrained velocity models extending over 2,000 km of island arc crust, shows that overall island arc crust is predominantly mafic. At depths greater than 8–10 km, i.e., confining pressures >0.2 GPa, arc crust is characterized by in situ seismic velocities greater than 6.5 km s^{-1}, clearly distinguishing it from typical continental crust (Fig. 4.15). Although felsic-intermediate rocks such as tonalite may be present over a broad depth range, such rocks can only predominate at depths less than 8 km; however, it is not possible to determine their proportion accurately at these relatively shallow depths, because the seismic velocities of mafic rocks can be significantly reduced by fluid-filled porosity.

In detail, island arc crust is characterized by its lateral variability, both across the arc as might be expected, but also along the arc. The crustal thickness of an island arc can be qualitatively related to the amount of extension it has undergone with the thickest 35 km island arc crust found in the Aleutian arc where extension has been minimal. The crust of the Izu arc, which has only been subject to removal of the Kyushu-Palau ridge from the rear arc thus limiting the volume of crust lost, is 26–35 km thick. In contrast the Bonin arc has been thinned by at least three episodes of extension, two of which did not lead to back-arc spreading, resulting in a 400 km wide arc and forearc with laterally variable 10–22 km thick crust. The average velocity profiles of other island arcs appear to lie between these end members, but the lower arc crust is not always well constrained in these other locations. Forearc crust commonly thins to 10–12 km close to the trench, but igneous crust as thick as 16 km has been observed in the Mariana and Bonin forearcs, suggesting that significant lateral variability can be present. Forearc crust can also thicken prior to collision through the accumulation of a thick sedimentary section derived from the approaching continent.

Arc crust can vary in thickness from 10–35 km over 300 km along strike, while the forearc can vary from 9–16 km over 50 km. Such changes in crustal thickness, and perhaps composition, due to an island arc's tectonic and magmatic evolution are likely to have a strong influence on the fashion in which arc–continent collision unfolds, resulting in significant along-strike variations in the character of preserved arc crust; for example, island arcs that have not been subject to extension are likely to have a relatively thick mafic middle and lower crust that may be less susceptible to obduction onto an incoming passive margin.

The seismic surveys reviewed here have been acquired using different parameters, especially numbers of recording seismometers, and analysed using different methodologies. The characteristics of the derived velocity models are a consequence of the methods used to produce them, with the assumption of lateral continuity often necessitated by a large receiver spacing. Comparisons of different island arc systems would be greatly facilitated by the use of similar, densely sampled acquisition geometries, which provide greater confidence in secondary phase identifications and permit the use of similar tomographic inversion techniques. 2D profiles across an arc are required to determine the broader tectonic setting and to allow estimation of magmatic flux from arc growth rates, but intriguing recent results have come from seismic profiles along arcs; strike profiles are an effective way of identifying both large-scale variations in arc structure and localised tectonic features that merit further detailed study. 3D surveys, which provide seismic velocity throughout a large crustal volume, can provide more robust estimates of arc growth, but at the cost of additional field effort.

The large-scale P wave velocity structure of many island arcs has been well determined over the last two decades. Looking forward, complementary S wave velocity models could help discriminate mafic and ultramafic lithologies in the lowermost arc crust (Behn and Keleman 2006). Seismic waveform inversion methods, which require an OBS spacing of ~1 km, can provide higher resolution velocity models, and have the potential to reveal the way tonalitic intrusions are distributed in the upper crust. Great progress has been made in understanding the seismic velocity structure of the lowermost arc crust and upper mantle wedge. However, combining a 3D active source survey with coincident passive recording where high levels of intraplate seismicity are present in a relatively shallowly subducting slab could generate the dense ray coverage necessary to refine velocity models at depths of 25–40 km, and better constrain deep magmatic processes. Coherent scattered noise and water-layer multiples usually obscure deep reflections, where present, in multichannel seismic profiles; progress on these two issues, which likely requires some form of 3D acquisition, might allow seismic reflection surveys to provide a complementary, higher resolution perspective on island arcs.

Acknowledgements I am very grateful to those who generously contributed seismic velocity models for this paper: G. Christeson, W. Crawford, S. Holbrook, S. Kodaira, E. Kurashimo, R. Larter, D. Lizarralde, S. Miura, A. Nishizawa, D. Shillington, N. Takahashi, and H. van Avendonk. Constructive reviews by Steve Holbrook and an anonymous reviewer plus comments from Sue DeBari improved the final manuscript. The bathymetry data for all the maps were obtained from the National Oceanic and Atmospheric Administration ETOPO1 global relief model (Amante and Eakins 2009). This project was supported by the Natural Sciences and Engineering Research Council of Canada.

Appendix

Table 4.1 lists the sections of the various wide-angle velocity models that were laterally averaged to create the 1D velocity-depth functions shown in Figs. 4.13 and 4.14. The x-coordinates correspond to those used originally in the publications cited. A maximum depth, below which the velocities are not considered well constrained, was chosen for each velocity function, and velocity functions are only displayed above these depths.

Representative 1D velocity depth functions for island arc crust were calculated by averaging the sections of the 2D arc velocity models listed in Table 4.1 (but excluding the continental part of Aleutian line A3) using three difference reference datums: mean sea level, the seafloor (taken to be the 1.52 km s^{-1} isovelocity contour), and the top of the igneous crust (Fig. 4.15). In many island arc settings, the top of the igneous crust is not well defined due to low velocity, high porosity volcanic rocks and intrusions into the overlying sedimentary section; so the 3.5 km s^{-1} contour was used to approximate this boundary. To obtain a 1D velocity model for a particular reference datum, e.g. the seafloor, each velocity model was depth-shifted so that the velocity value immediately below the datum was aligned at zero across the 2D model. This results in higher velocities at zero depth than the selected datum value due to discretization of the velocity models. All the 2D models were then averaged. The contribution of a particular velocity model to the average velocity functions depends on the length of the model in Table 4.1. Thus the long-strike lines along the Aleutian and Izu, Bonin and Mariana contribute more to the average than relatively short dip lines, such as that across South Sandwich arc.

Table 4.1 Locations of derived 1D velocity-depth functions

Arc	Profile	Xmin	Xmax	Xmax-Xmin	Zmax	References
Aleutian	A1 – Dip	234	269	35	31	Holbrook et al. (1999)
Aleutian	A2 – Strike	180	750	570	38	Shillington et al. (2004)
Aleutian	A3 – Dip-Cont	235	275	40	35	Lizarralde et al. (2002)
Aleutian	A3 – Dip-Ocean	219	255	36	35	Lizarralde et al. (2002)
Bonin	Dip	340	380	40	25	Takahashi et al. (2009)
Bonin	Strike	700	950	250	23	Kodaira et al. (2007b)
Izu	Dip	150	250	100	19	Suyehiro et al. (1996)
Izu	Strike	150	450	300	38	Kodaira et al. (2007a)
L. Antilles	Dip	40	65	25	27	Christeson et al. (2008)
Mariana	Dip	185	215	30	35	Takahashi et al. (2007)
Mariana	Strike – Modern	80	250	170	24	Calvert et al. (2008)
Mariana	Strike – Eocene	100	360	260	27	Calvert et al. (2008)
Solomon	Dip	260	280	20	14	Miura et al. (2004)
S. Sandwich	Dip	300	320	20	15	Brugier and Larter (2001)
Tonga	Dip	50	140	90	14	Crawford et al. (2002)
Remnant Arc						
Kyushu Palau	Dip – KPr20	69	81	22	18	Nishizawa et al. (2007)
Kyushu Palau	Dip – SPr5	38	52	14	20	Nishizawa et al. (2007)
West Mariana	Dip	−105	−70	35	26	Takahashi et al. (2007)

Table 4.2 Reference 1D velocity-depth functions for island arcs (km s^{-1})

Depth (km)	Velocity below mean sea level	Standard deviation	Velocity below seafloor	Standard deviation	Velocity below top igneous crust	Standard deviation
0	1.503	0.024	3.249	1.648	4.730	1.047
1	2.649	1.496	4.438	1.322	5.265	0.740
2	3.795	1.781	5.054	0.960	5.652	0.511
3	4.561	1.398	5.505	0.654	5.940	0.360
4	5.180	0.952	5.828	0.452	6.160	0.281
5	5.587	0.667	6.085	0.332	6.306	0.261
6	5.888	0.487	6.259	0.278	6.433	0.277
7	6.106	0.365	6.410	0.295	6.581	0.274
8	6.279	0.269	6.584	0.299	6.689	0.286
9	6.481	0.284	6.672	0.286	6.788	0.268
10	6.586	0.254	6.770	0.263	6.848	0.277
11	6.681	0.233	6.838	0.268	6.901	0.286
12	6.786	0.196	6.896	0.281	6.954	0.296
13	6.855	0.210	6.953	0.290	7.002	0.308
14	6.926	0.235	6.990	0.308	7.040	0.316
15	6.968	0.251	7.037	0.322	7.085	0.329
16	7.011	0.268	7.082	0.329	7.131	0.332
17	7.060	0.287	7.130	0.330	7.115	0.235
18	7.104	0.299	7.202	0.318	7.193	0.232
19	7.170	0.286	7.198	0.235	7.239	0.234
20	7.259	0.291	7.232	0.238	7.235	0.211
21	7.303	0.289	7.222	0.215	7.266	0.216
22	7.342	0.291	7.255	0.218	7.296	0.223
23	7.298	0.241	7.285	0.226	7.270	0.226
24	7.332	0.249	7.326	0.237	7.297	0.232
25	7.329	0.256	7.282	0.228	7.329	0.248
26	7.336	0.246	7.310	0.237	7.361	0.265
27	7.364	0.251	7.343	0.256	7.408	0.267

(*continued*)

Table 4.2 (continued)

Depth (km)	Velocity below mean sea level	Standard deviation	Velocity below seafloor	Standard deviation	Velocity below top igneous crust	Standard deviation
28	7.336	0.256	7.373	0.270	7.435	0.275
29	7.373	0.269	7.420	0.270	7.460	0.285
30	7.403	0.281	7.446	0.279	7.457	0.269
31	7.429	0.291	7.446	0.264	7.477	0.276
32	7.477	0.289	7.463	0.270	7.337	0.173
33	7.497	0.295	7.511	0.327	7.468	0.368
34	7.536	0.330	7.582	0.428	7.754	0.405
35	7.633	0.378	7.903	0.312	7.974	0.215
36	7.769	0.363	7.978	0.211		
37	7.933	0.205				
38	7.976	0.213				

References

Amante C, Eakins BW (2009) Arc-minute global relief model: procedures, data sources and analysis. Technical memorandum NESDIS NGDC-24, NOAA, Boulder

Arai T (1987) Tectonics of Tanzawa mountains: constraints from metamorphic petrology. J Geol Soc Jpn 93:185–200

Bard JP, Maluski P, Matte P et al (1980) The Kohistan sequence, crust and mantle of an obducted island arc. Geol Bull Univ Peshawar 13:87–94

Behn MD, Keleman PB (2003) Relationship between P-wave velocity and the composition of anhydrous igneous and meta-igneous rocks. Geochem Geophys Geosyst. doi:10.1029/2002GC000393

Behn MD, Keleman PB (2006) Stability of arc lower crust: Insights from the Talkeetna arc section, south central Alaska, and the seismic structure of modern arcs. J Geophys Res. doi:10.1029/2006JB004327

Bibee LD, Shor GG Jr, Lu RS (1980) Inter-arc spreading in the Mariana Trough. Mar Geol 35:183–197

Birch F (1943) Elasticity of igneous rocks at high temperatures and pressures. Geol Soc Am Bull 54:263–286

Bouysse P (1988) Opening of the Grenada back-arc basin and evolution of the Caribbean Plate during the Mesozoic and early Paleogene. Tectonophysics 149:121–143

Boynton CH, Westbrook GK, Bott, MHP et al (1979) A seismic refraction investigation of crustal structure beneath the Lesser Antilles island arc. Geophys JR astr Soc 58: 371–393

Brocher TM (2005) Empirical relations between elastic wavespeeds and density in the Earth's crust. Bull Seismol Soc Am 95:2081–2092

Brugier N, Larter R (2001) Crustal structure and rate of growth of the South Sandwich arc from wide-angle seismic data. Eur Union Geosc Prog Abs 392–393

Burke K (1988) Tectonic evolution of the Caribbean. Annu Rev Earth Planet Sci 16:201–230

Calvert AJ, Klemperer SL, Takahashi N et al (2008) Three-dimensional crustal structure of the Mariana island arc from seismic tomography. J Geophys Res. doi:10.1029/2007JB004939

Card KD (1990) A review of the Superior Province of the Canadian Shield, a product of Archean accretion. Precambrian Res 48:99–156

Christensen NI (1979) Compressional wave velocities in rocks at high temperatures and pressures, critical thermal gradients, and crustal low velocity zones. J Geophys Res 84: 6849–6857

Christensen NI, Mooney WD (1995) Seismic velocity structure and composition of the continental crust. J Geophs Res 100: 9761–9788

Christeson G, Mann P, Escalona A et al (2008) Crustal structure of the Caribbean – northeastern South America arc-continent collision zone. J Geophys Res. doi:10.1029/2007JB005373

Clift P, Vannucchi P (2004) Controls on tectonic accretion versus erosion in subduction zones: implications for the origin and recycling of the continental crust. Rev Geophys. doi:10.1029/2003RG000127

Cook FA, Clowes RM, Snyder DB et al (2004) Precambrian crust beneath the Mesozoic northern Canadian Cordillera discovered by Lithoprobe seismic reflection profiling. Tectonics. doi:10.1029:2002TC001412

Crawford AJ, Beccaluva L, Serri G (1981) Tectono-magmatic evolution of the West Philippine-Mariana region and the origin of boninites. Earth Planet Sci Lett 54:346–356

Crawford WC, Hidebrand JA, Dorman LM, Webb SC, Wiens DA (2002) Tonga Ridge and Lau Basin crustal structure from seismic refraction data. J Geophys Res. doi:10.1029/2001JB001435

d'Ars JB, Jaupart C, Sparks RSJ (1995) Distribution of volcanoes in active margins. J Geophys Res 100:20421–20432

DeMets C, Dixon TH (1999) New kinematic models for Pacific-North America plate motion from 3 Ma to present: I. Evidence for steady motion and biases in the NUVEL-1A model. Geophys Res Lett 26:1921–1924

Dimalanta C, Taira A, Yumul GP Jr et al (2002) New rates of western Pacific island arc magmatism from seismic and gravity data. Earth Planet Sci Lett 202:105–115

Fliedner MM, Klemperer SK (1999) Structure of an island-arc: wide-angle studies in the eastern Aleutian Islands, Alaska. J Geophys Res 104:10667–10694

Fryer P (1995) Geology of the Mariana Trough. In: Taylor B (ed) Back-arc basins: tectonics and magmatism. Plenum, New York

Fujie G, Ito A, Kodaira S et al (2006) Confirming sharp bending of the Pacific plate in the northern Japan trench subduction zone by applying a travel time mapping method. Phys Earth Planet Int 157:72–85

Garrido CJ, Bodinier J-L, Burg J-P et al (2006) Petrogenesis of mafic garnet granulite in the lower crust of the Kohistan paleo-arc complex (Northern Pakistan): implications for intra-crustal differentiation of island arcs and generation of continental crust. J Petrol 47:1873–1914

Geist EL, Childs JR, Scholl DW (1988) The origin of summit basins of the Aleutian Ridge: implications for block rotation of an arc massif. Tectonics 7:327–342

Gill JB (1981) Orogenic andesites and plate tectonics. Springer, Berlin

Gorshkov GS (1970) Volcanism and the upper mantle. Plenum, New York

Grow JA (1973) Crustal and upper mantle structure of the central Aleutian arc. Geol Soc Am 84:2169–2192

Hoffman PF (1989) Precambrian geology and tectonic history of North America. In: Bally AW, Palmer PR (eds) The Geology of North America: an Overview, vol A. Geol Soc Am, Boulder

Holbrook WS, Lizarralde D, McGeary S et al (1999) Structure and composition of the Aleutian island arc and implications for continental growth. Geology 27:31–34

Hole JA (1992) Nonlinear high-resolution three-dimensional seismic travel time tomography. J Geophys Res 97: 6553–6562

Hole JA, Zelt BC (1995) 3-D finite-difference reflection travel times. Geophys J Int 121:427–434

Hussong DM, Uyeda S (1981) Tectonic processes and the history of the Mariana arc, a synthesis of the results of Deep Sea Drilling Project Leg 60. In: Hussong DM (ed) Initial Reports of the Deep Sea Drilling Project, Vol 60. Ocean Drilling Program, College Station

Hyndman RD, Shearer PM (1989) Water in the lower continental crust – modelling magnetotelluric and seismic reflection results. Geophys J Int 98:343–365

Ishizuka O, Kimura J, Li YB et al (2006) Early stages in the evolution of Izu-Bonin arc volcanism: new age, chemical, and isotopic constraints. Earth Planet Sci Lett 250:385–401

Ito A, Fujie G, Kodaira S et al (2005) Bending of the subducting oceanic plate and its implication for rupture propagation of large interplate earthquakes off Miyagi, Japan, in the Japan trench subduction zone. Geophys Res Lett. doi:10.1029/2004GL022307

Iturrino GJ, Christensen NI, Kirby S, Salisbury MH (1991) Seismic velocities and elastic properties of oceanic gabbroic rocks from Hole 735B. Proc Ocean Drill Program Sci Results 118:227–244

Iturrino GJ, Miller DJ, Christensen NI (1996) Velocity behavior of lower crustal and upper mantle rocks from a fast-spreading ridge at Hess Deep. Proc Ocean Drill Program Sci Results 147:417–440

Jacob KH, Hamada K (1972) The upper mantle beneath the Aleutian island arc from pure-path Rayleigh-wave dispersion data. Bull Seismol Soc Am 62:1439–1454

Jarrard RD (1986) Relations among subduction parameters. Rev Geophys 24:217–284

Karig DE (1970) Ridges and basins of the Tonga-Kermadec island arc system. J Geophys Res 75:239–254

Kawate S, Arima M (1998) Petrogenesis of the Tanzawa plutonic complex, central Japan: exposed felsic crust of the Izu-Bonin-Mariana arc. Island Arc 7:342–358

Kern H (1978) The effect of high temperature and high confining pressure on compressional wave velocities in quartz-bearing and quartz-free igneous and metamorphic rocks. Tectonophysics 44:185–203

Kitamura K, Ishikawa M, Arima M (2003) Petrological model of the northern Izu-Bonin-Mariana arc crust: constraints from high pressure measurements of elastic wave velocities of the Tanzawa plutonic rocks, central Japan. Tectonophysics 371:213–221

Kobayashi KS, Kasuga S, Kl O (1995) Shikoku Basin and its margins. In: Taylor B (ed) Back-arc basins: tectonics and magmatism. Plenum, New York

Kodaira S, Sato T, Takahashi N et al (2007a) Seismological evidence for variable growth of crust along the Izu intraoceanic arc. J Geophys Res. doi:10.1029/2006JB004593

Kodaira A, Sato T, Takahashi N et al (2007b) New seismological constraints on growth of continental crust in the Izu-Bonin intra-oceanic arc. Geology 35:1031–1034

Kono Y, Ishikawa M, Harigane Y et al (2009) P- and S-wave velocities of the lowermost crustal rocks from the Kohistan arc: implications for seismic Moho discontinuity attributed to abundant garnet. Tectonophysics 467:44–54

Korenaga J, Kelemen PB, Holbrook WS (2002) Methods for resolving the origin of large igneous provinces from crustal seismology. J Geophys Res. doi:10.1029/2001JB001030

Kusznir, NJ, Park RG (1987) The extensional strength of the continental lithosphere: its dependence on geothermal gradient, and crustal composition and thickness. In: Coward MP, Dewey JF, Hancock, PL (eds) Continental extensional tectonics. Geol Soc, London.

Larner K, Chambers YM et al (1983) Coherent noise in marine seismic data. Geophysics 48:854–886

Leat PT, Larter RD (2003) Intra-oceanic subduction systems: introduction. In: Larter RD, Leat PT (eds) Intra-oceanic subduction systems: tectonic and magmatic processes, vol 219, Geol Soc Lon Spec Pub., pp 1–17

Lizarralde D, Holbrook WS, McGeary S et al (2002) Crustal structure of a volcanic arc, wide-angle results from the western Alaska Peninsula. J Geophys Res. doi:10.1029/2001JB000230

Malfait BT, Dinkelman MG (1972) Circum-Caribbean tectonic and igneous activity and the evolution of the Caribbean plate. Geol Soc Am Bull 83:251–271

Martinez F, Taylor B (2006) Modes of crustal accretion in back-arc basins: Inferences from the Lau Basin. In: Christie DM et al (eds) Back-arc spreading systems: Geological, biological, chemical and physical interactions. Am Geophys Union, Washington

Miller DJ, Christensen NI (1994) Seismic signature and geochemistry of an island arc: a multidisciplinary study of the Kohistan accreted terrane, northern Pakistan. J Geophys Res 99:11623–11642

Miura S, Suyehiro K, Takahashi N et al (2004) Seismological structure and implications of collision between the Ontong Java plateau and Solomon island arc from ocean bottom seismometer-airgun data. Tectonophysics 389: 191–220

Molnar P, Atwater T (1978) Interarc spreading and Cordilleran tectonics as alternatives related to the age of subducted oceanic lithosphere. Earth Planet Sci Lett 41:330–340

Murauchi S, Den N, Asano S et al (1968) Crustal structure of the Philippine Sea. J Geophys Res 73:3143–3171.

Nakajima K, Arima M (1998) Melting experiments on hydrous low-K tholeiite: implications for the genesis of tonalitic crust in the Izu-Bonin-Mariana arc. Island Arc 7:359–373

Nishizawa A, Kaneda K, Katagiri Y et al (2007) Variation in crustal structure along the Kyushu-Palau Ridge at 15–21°N on the Philippine Sea plate based on seismic refraction profiles. Earth Planets Space 59:e17–e20

Nitsuma N (1989) Collision tectonics in the South Fossa Magna, Central Japan. Mod Geol 14:3–18

Oakley AJ, Taylor B, Moore GF, Gooliffe A (2009) Sedimentary, volcanic, and tectonic processes of the central Mariana Arc: Mariana Trough back-arc basin formation and the West Mariana Ridge. Geochem Geophys Geosyst. doi:10.1029/2008GC002312

Okino K, Shimakawa Y, Nagaoka S (1994) Evolution of the Shikoku Basin. J Geomagn Geoelectr 46:463–479

Okino K, Ohara Y, Kasuga S et al (1999) The Philippine Sea: new survey results reveal the structure and the history of the marginal basins. Geophys Res Lett 26:2287–2290

Plafker G, Berg HC (1994) Overview of the geology and tectonic evolution of Alaska. In: Plafker G, Berg HC (eds) The Geology of North America, vol G-1, The Geology of Alaska. Geol Soc Am, Boulder

Plafker G, Moore JC, Winkler GR (1994) Geology of the southern Alaska margin. In: Plafker G, Berg HC (eds) The Geology of North America, vol G-1, The Geology of Alaska. Geol Soc Am, Boulder

Rudnick LR, Fountain MD (1995) Nature and composition of the continental crust: a lower crustal perspective. Rev Geophys 33:267–309

Sato T, Kodaira S, Takahashi N et al (2009) Amplitude modeling of the seismic reflectors in the crust-mantle transition layer beneath the volcanic front along the northern Izu-Bonin island arc. Geochem Geophys Geosyst. doi:10.1029/2008GC001990

Scholl DW, Stevenson AJ, Mueller S et al (1992) Exploring the notion that southeast-Asian-type escape tectonics and trench clogging are involved in regional-scale deformation of Alaska and the formation of the Aleutian-Bering sea region. In: Flower M, McCabe R, Hilde T (eds) Southeast Asia structure, tectonics and magmatism, Proc Geod Res Inst Symp. Texas A&M Univ, College Station

Seno T, Stein S, Gripp AE (1993) A model for the motion of the Philippine Sea plate consistent with NUVEL and geological data. J Geophys Res 98:17941–17948

Shillington DJ, van Avendonk HJA, Holbrook WS et al (2004) Composition and structure of the central Aleutian island arc from arc-parallel wide-angle seismic data. Geochem Geophys Geosyst. doi:10.1029/2004GC000715

Shor GG Jr, Kirk HK, Menard HW (1971) Crustal structure of the Melanesian area. J Geophys Res 76:2562–2586

Speed RC, Walker JA (1991) Oceanic crust of the Grenada basin in the southern Lesser Antilles arc platform. J Geophys Res 96:3835–3851

Stern RJ (2002) Subduction zones. Rev Geophys. doi:10.1029/2001RG000108

Stern RJ, Bloomer SH (1992) Subduction zone infancy: examples from the Eocene Izu-Bonin-Mariana and Jurassic California arcs. Geol Soc Am Bull 104:1621–1636

Stern RJ, Fouch MJ, Klemperer SL (2003) An overview of the Izu-Bonin-Mariana subduction factory. In: Eiler JM (ed) Inside the subduction factory. Am Geophys Union, Washington

Suyehiro K, Takahashi N, Ariie Y et al (1996) Continental crust, crustal underplating, and low-Q upper mantle beneath an island arc. Science 272:390–392

Takahashi N, Suyehiro K, Shinohara M (1998) Implications from the seismic crustal structure of the northern Izu-Bonin arc. Island Arc 7:383–394

Takahashi N, Kodaira S, Klemperer S et al (2007) Crustal structure and evolution of the Mariana intra-oceanic island arc. Geology 35:203–206

Takahashi N, Kodaira S, Tatsumi Y et al (2008) Structure and growth of the Izu-Bonin-Mariana arc crust: 1. Seismic constraint on crust and mantle structure of the Mariana arc–back-arc system. J Geophys Res. doi:10.1029/2007JB005120

Takahashi N, Kodaira S, Tatsumi Y et al (2009) Structural variations of arc crusts and rifted margins in the southern Izu-Ogasawara arc-back arc system. Geochem Geophys Geosyst. doi:10.1029/2008GC002146

Tani K, Dunkley DJ, Kimura J-I et al (2010) Syncollisional rapid granitic magma formation in an arc-arc collision zone: evidence from the Tanzawa plutonic complex, Japan. Geology 38:215–218

Tatsumi Y, Tani K, Kogiso T et al (2008) Structure and growth of the Izu-Bonin-Mariana arc crust: 2. Arc evolution, continental crust formation, and crust-mantle transformation. J Geophys Res. doi:10.1029/2007JB005121

Taylor B (1992) Rifting and volcano-tectonic evolution of the Izu-Bonin-Mariana arc. In: Maddox E (ed) Proceedings of the ocean drilling program, scientific results, Vol 126. Ocean Drilling Program, College Station

Taylor B, Karner GD (1983) On the evolution of marginal basins. Rev Geophys Space Phys 21:1727–1741

Uyeda S, Kanamori H (1979) Back-arc opening and the mode of subduction. J Geophys Res 84:47–56

Van Avendonk HJA, Shillington DJ, Holbrook WS, Hornbach MJ (2004) Inferring crustal structure in the Aleutian island arc from a sparse wide-angle seismic data set. Geochem Geophys Geosyst. doi:10.1029/2003GC000664

Von Huene R, Scholl DW (1991) Observations at convergent margins concerning sediment subduction, subduction erosion, and the growth of continental crust. Rev Geophys 29: 279–316

White RS (1984) Atlantic oceanic crust: Seismic structure of a slow-spreading ridge. In: Gass IG (ed) Ophiolites and oceanic lithosphere, vol 13. Geol Soc Lon, London

Wiebenga WA (1973) Crustal structure of the New Britain-New Zealand region. In: Coleman PJ (ed) The Western Pacific. Western Australia University Press, Perth

Yamamoto Y, Kawakami S (2005) Rapid tectonics of the late Miocene Boso accretionary prism related to the Izu-Bonin arc collision. Island Arc 14:178–198

Zelt CA, Barton PJ (1998) 3-D seismic refraction tomography: a comparison of two methods applied to data from the Faroes Basin. Geophys J Int 103:7187–7210

Zelt CA, Smith RB (1992) Seismic traveltime inversion for 2-D crustal velocity structure. Geophys J Int 108:16–34